Improving Global Analysis and Short-Range Forecast Using Rainfall and Moisture Observations Derived from TRMM and SSM/I Passive Microwave Instruments

Arthur Y. Hou[*], Sara Q. Zhang[+], Arlindo M. da Silva,[*]
William S. Olson[#], Christian D. Kummerow[*], Joanne Simpson[*]

Manuscript for
Bulletin of the American Meteorological Society
May 22, 2000

[*]National Aeronautics and Space Administration/Goddard Space Flight Center, Greenbelt, Maryland.
[+]General Sciences Corp., a subsidiary of Science Applications International Corp., Beltsville, Maryland.
[#]University of Maryland Baltimore County, Baltimore, Maryland.

Corresponding author address: Dr. Arthur Y. Hou, Code 910.3, NASA Goddard Space Flight Center, Greenbelt, MD, 20771. E-mail: arthur.hou@gsfc.nasa.gov

Abstract

The Global Precipitation Mission, a satellite project under consideration as a follow-on to the Tropical Rainfall Measuring Mission (TRMM) by the National Aeronautics and Space Agency (NASA) in the United States, the National Space Development Agency (NASDA) in Japan, and other international partners, comprises an improved TRMM-like satellite and a constellation of 8 satellites carrying passive microwave radiometers to provide global rainfall measurements at 3-hour intervals. The success of this concept relies on the merits of rainfall estimates derived from passive microwave radiometers. This article offers a proof-of-concept demonstration of the benefits of using rainfall and total precipitable water (TPW) information derived from such instruments in global data assimilation with observations from the TRMM Microwave Imager (TMI) and 2 Special Sensor Microwave/Imager (SSM/I) instruments.

Global analyses that optimally combine observations from diverse sources with physical models of atmospheric and land processes can provide a comprehensive description of the climate systems. Currently, such data analyses contain significant errors in primary hydrological fields such as precipitation and evaporation, especially in the tropics. We show that assimilating the 6-h averaged TMI and SSM/I surface rainrate and TPW retrievals improves not only the hydrological cycle but also key climate parameters such as clouds, radiation, and the upper tropospheric moisture in the analysis produced by the Goddard Earth Observing System (GEOS) Data Assimilation System, as verified against radiation measurements by the Clouds and the Earth's Radiant Energy System (CERES) instrument and brightness temperature observations by the TIROS Operational Vertical Sounder (TOVS) instruments.

Typically, rainfall assimilation improves clouds and radiation in areas of active convection, as well as the latent heating and large-scale motions in the tropics, while TPW assimilation leads to reduced moisture biases and improved radiative fluxes in clear-sky regions. Ensemble forecasts initialized with analyses that incorporate TMI and SSM/I rainfall and TPW data also yield better short-range predictions of geopotential heights, winds, and precipitation in the tropics. This study offers a compelling illustration of the potential of using rainfall and TPW information derived from passive microwave instruments to significantly improve the quality of 4-dimensional global datasets for climate analysis and weather forecasting applications.

1. Introduction

Understanding the Earth's climate and how it responds to climate perturbations relies on what we know about how atmospheric moisture, clouds, latent heating, and the large-scale circulation vary with changing climatic conditions. The physical process that links these key climate elements is precipitation, which directly affects the generation of clouds and large-scale motions and thus indirectly influences the distribution of moisture and the greenhouse warming in the earth's atmosphere. A quantitative understanding of these precipitation-related processes and their dependence on the atmospheric state is crucial to developing the capability to model and predict climate change with confidence. The present-day knowledge of rainfall distribution and variability is very limited, especially over the oceans and in the tropics. Space-borne rainfall sensors are essential tools for advancing our understanding of the earth's water and energy cycles.

The Tropical Rainfall Measuring Mission (TRMM) is a joint satellite project between the National Aeronautics and Space Agency (NASA) of the United States and the National Space Development Agency (NASDA) of Japan. TRMM was designed to measure rainfall in the tropics and subtropics using a precipitation radar (PR) and the TRMM Microwave Imager (TMI) (TRMM 1996). Coincident measurements by the PR and TMI provide cross-validation to improve the accuracy of rainrate estimation and physical interpretations of radiometer data. The TRMM satellite was launched into a non-sun-synchronous orbit of inclination of 35° on Thanksgiving Day in 1997. The TMI is similar in design to the Special Sensor Microwave/Imager (SSM/I) instrument but with an additional 10.65 GHz channel and a slightly modified water vapor channel. The TMI rainfall and total precipitable water (TPW) observations may be combined with similar retrievals derived from the SSM/I instruments aboard the sun-synchronous, polar-orbiting satellites operated by the Defense Meteorological Satellite Program (DMSP) to improve the spatial and temporal coverage and reduce sampling errors. But the combined TMI and the present-day SSM/I observations do not fully capture the rapid temporal and spatial variations of the precipitation process. Currently in the planning stage is a Global Precipitation Mission (GPM), a multi-national satellite project based on an improved TRMM-like satellite and a constellation of 8 satellites carrying passive microwave radiometers to provide global rainfall coverage (75°S to 75°N) at 3-hour intervals. The success of this GPM concept relies upon the

merits of precipitation estimates derived from passive microwave radiometers.

In this proof-of-concept study we seek to demonstrate the benefits of using rainfall and TPW retrievals derived from passive microwave instruments in global data assimilation, even with the limited coverage afforded by three satellites. Four-dimensional (4D) global data assimilation that optimally combines observations from diverse sources with physical models of the earth system aims to provide time-continuous, physically-consistent, gridded datasets useful for studying the interactions between the hydrological cycle, atmospheric dynamics, and climate variability. To do so, the assimilation must be quantitatively accurate in depicting the precipitation intensity and variability since many key climate parameters such as clouds and radiation are directly affected by the precipitation process. At the present time, the utility of global reanalyses produced using fixed assimilation systems is limited by significant errors in the primary hydrological fields such as precipitation, evaporation, especially in the tropics, where conventional observations are sparse (WCRP 1998, Newman et al. 2000).

Operational centers currently do not use precipitation data to produce forecasts or analysis products. However, there have been abundant studies showing that assimilation of satellite-based rainfall estimates can improve numerical weather prediction and data analysis (e.g., Krishnamurti et al. 1984, 1991, 1993; Donner 1988; Puri and Miller 1990; Turpeinen et al. 1990; Kasahara et al. 1994, Zupanski and Mesinger 1995, Treadon 1996, Tsuyuki 1996a, 1996b, 1997). Most investigations focused on using precipitation data to improve short-range forecasts and the first-guess fields used in data analyses. But, in the presence of systematic errors in the forecast model, forecast improvements may not be indicative of the extent of the improvements that can be achieved in the time-averaged assimilation fields or in terms of the quality of reanalyses as 4D climate datasets. In two separate studies - one using SSM/I-derived rainfall and TPW retrievals available prior to the TRMM launch and the other using TMI data, Hou et al. (2000a, 2000b) showed that assimilating the 6-h averaged tropical rainfall and TPW retrievals from these instruments improves not only short-range forecasts but is even more effective in reducing systematic errors in the hydrological cycle and key climate parameters such as clouds and atmospheric radiation in the assimilated dataset produced by the Goddard Earth Observing System (GEOS) Data Assimilation System (DAS). These studies show that physically-based rainfall estimates derived from microwave instruments, despite some uncertainty in the retrieved

intensity and the limited observations available in a 6-h analysis window, do provide valuable information that can be used to good advantage in data assimilation.

In this article we show the benefits of increased data coverage in assimilating the combined rainfall and TPW retrievals from the TMI and 2 SSM/I instruments aboard the DMSP *F13* and *F14* satellites. The work demonstrates the potential of using these data types to improve forecasts and generate analyses capable of providing quantitatively accurate descriptions of rainfall and latent heating variations for studying the role of the global water cycle in climate. In Sec. 2, we discuss the need for better precipitation analyses and more robust metrics for assessing the consequence of inaccurate rainfall in global analyses. Section 3 describes the precipitation and TPW retrieval products used in the study. Section 4 describes the rainfall/TPW assimilation algorithm and experiments. Section 5 analyzes the impact of rainfall/TPW assimilation on the time-averaged fields in the GEOS analysis. Section 6 discusses the impact on short-range forecasts. Section 7 summarizes the main findings and discusses future developments.

2. Background

Global reanalyses currently yield precipitation estimates that differ quantitatively from each other and from observation-based estimates such as the combined satellite-gauge rainrates from the Global Precipitation Climatology Project (GPCP) (Adler et al. 1996, Huffman et al. 1997) or the combined rainrates derived from the TRMM and geostationary satellites (Sorooshian et al. 1999). The discrepancies are especially pronounced in the tropics, where the conventional observation network is sparse and rainfall analyses are typically model-generated quantities sensitive to the physical parameterization scheme employed by the assimilation system. However, the present-day rainfall observations also suffer from uncertainties in retrieval algorithms and inadequate sampling. They provide but an estimate of the truth. The lack of definitive rainrate estimates has hindered efforts to quantify precipitation errors in global analyses and obscured the penalty for incurring such errors. To make progress, we need to establish, if possible, that the observed precipitation, though imperfect, is, in fact, more accurate than the model-generated estimates. We also need to make use of independent observations with higher accuracies to

quantify the errors in assimilated data associated with precipitation errors.

Based on physical principles and observations, we know that many key climate parameters such as clouds and radiation are directly linked to precipitation processes. For instance, satellite observations of the 1987-88 El Niño Southern Oscillation (ENSO) event show that the change in the July-mean GPCP precipitation in the tropics is spatially correlated (with coefficients greater than 0.7) with changes in the high-cloud fraction from the International Satellite Cloud Climatology Project (ISCCP) and the top-of-the-atmosphere (TOA) radiative fluxes from the Earth Radiation Budget Experiment (ERBE) (see TRMM Data Assimilation at NASA Goddard 2000). Regions of enhanced convection are associated with increased cloud cover, less shortwave heating and less outgoing longwave radiation (OLR). The close links between these fields suggest that radiation measurements from space-borne instruments can provide an indirect but effective means for estimating precipitation errors in global analyses, given that uncertainties in radiation measurements are generally much less than that in satellite-based precipitation estimates.

The metrics we use in this study to assess the impact of rainfall/TPW assimilation on the quality of the GEOS analysis consist of: (i) evaluating the OLR and outgoing shortwave radiation (OSR) from the assimilation against measurements by the Clouds and the Earth's Radiant Energy System (CERES) instrument aboard the TRMM satellite, and (ii) comparing the computed synthetic brightness temperatures for TIROS Operational Vertical Sounder (TOVS) spectral channels that are sensitive to moisture with TOVS observations. The CERES/TRMM and TOVS observations can both serve as independent data for verification since neither was assimilated in the GEOS DAS. In terms of the monthly-mean tropical precipitation, current reanalyses all have order-one discrepancies from the combined satellite-gauge GPCP estimate (see TRMM Data Assimilation at NASA Goddard 2000). These discrepancies are typically of the size as the signals. In Sec. 5 we show that as we assimilate the TMI and SSM/I rainrates and TPW data to bring the tropical precipitation in the GEOS analysis into better quantitative agreement with the GPCP estimate, errors in the TOA radiative fluxes w.r.t. the CERES measurements become substantially reduced. This indicates that the satellite-based precipitation estimates are more consistent with the CERES/TRMM radiation measurements than the predominantly model-generated rainfall analysis without the benefit of satellite precipitation data.

3. TMI and SSM/I-Derived Precipitation and TPW Retrievals

a. GPROF TMI and SSM/I precipitation retrievals

The surface precipitation data used in this study are physical retrievals from TMI and SSM/I radiance measurements using the Goddard Profiling (GPROF) Algorithm, which derives rainrates and precipitation vertical structure from microwave radiometer and/or radar measurements (Kummerow et al. 1996, Olson et al. 1996) using a Bayesian technique similar to the algorithms developed by Pierdicca et al. (1996) and Haddad et al. (1997). The GPROF scheme uses a database of simulated precipitation vertical profiles and the associated microwave radiances generated by cloud-resolving model coupled to a radiative transfer code. This database serves as a "reference library" to which actual sensor-observed radiances can be compared. Given a set of multichannel radiance observations from a particular sensor, the entire library of simulated radiances is scanned; the "retrieved" profile is a composite using profiles stored in database which correspond to simulated radiances consistent with the observed radiances.

The TMI and SSM/I rain estimates are derived from essentially the same algorithm, but modified for the different channel selection and resolution of the two instruments. Because the TMI has greater than twice the spatial resolution of the SSM/I, rain estimates from TMI exhibit a greater dynamic range than those from SSM/I; however, space-time average estimates from SSM/I and TMI are usually within about 10%. Comparison of zonally-averaged monthly-mean rainrates from SSM/I (DMSP *F13* and *F14*) and TMI at 2.5° latitude resolution shows that the TMI and SSMI/I rainrates are generally very close, with the peak rainrates associated with the Inter-Tropical Convergence Zone differing by at most 10%, despite the different diurnal sampling of the SSM/I and TMI over a month. For assimilation into the GEOS DAS, the single-footprint, instantaneous GPROF TMI and SSM/I surface rainrates are horizontally averaged to 2° latitude by 2.5° longitude grids, then time-averaged over 6 hours centered at analysis times (0000, 0600, 1200, 1800 UTC).

The random error of each GPROF-retrieved rainrate may be estimated by evaluating the local variance of rainrates in the model database about the retrieved rainrate (Olson et al. 1996). According to this method, the random error of single-footprint, instantaneous rainfall rates is

estimated to be ~100% of the retrieved rainrate. But the instantaneous gridded rainrates have relatively low random error since the pixels completely cover a 2° x 2.5° gridbox in a full-view overpass. Over each 2° x 2.5° gridbox, approximately 1000 single-footprint TMI estimates are used to compute the area-average, instantaneous rainrate. Following the analysis of Bell et al. (1990), the corresponding random error of the gridbox-averaged TMI rainrate is about 20%, without accounting for possible inte-footprint correlations of errors. Undersampling of the time-average rainrate over each 6-h analysis interval contributes additional error, approximately 20-60%, depending upon the number of TMI overpasses within the interval. One complication in this estimate is that the relative (percent) random error varies roughly as the inverse square root of the rainrate, so that estimates of relative random errors significantly worse in light rain areas, but better in heavy rain areas (Huffman 1997).

The global bias is not yet established for GPROF rainfall estimates since most regions lack the necessary validation data and no statistical model has been developed to estimate bias from other parameters. A recent intercomparison of TMI GPROF and coincident space-borne Precipitation Radar estimates of rainrate suggests biases on the order of 30% over land and ocean in terms of the annual mean (Kummerow et al. 2000). In this study we assimilate the 6-h gridded TMI and SSM/I surface rainrates between 30°S and 30°N over both the oceans and land. Although microwave-based rainfall estimates tend to be less accurate over land, our results will show that assimilating the GPROF rainrates over land greatly improves precipitation over continents w.r.t. the gauge-based GPCP estimates.

b. Wentz retrievals of total precipitable water

The TPW data are retrievals from TMI and SSM/I observations over oceans using essentially the same algorithms (Wentz 1997), except for adjustments to account for small differences in GHz between the TMI and SSM/I channels and the TMI water vapor being measured at 21 GHz rather than 22.235 GHz as in SSM/I. The TMI and SSM/I TPW data are available online from the Remote Sensing System (RSS 2000) in the form of maps of ascending and descending orbit segments at a pixel resolution of 25 km. The rms accuracy of the SSM/I TPW retrieval is about 1 mm, with the accuracy of the TMI TPW retrieval expected to be

comparable or better. These high-resolution data with good quality flags are then processed to produce 6-hour average 2° x 2.5° gridded TPW data for ingestion into the GEOS DAS.

4. Assimilation Methodology and Experiments

The algorithm we use to assimilate surface rainfall and TPW retrievals in the GEOS DAS is a variational procedure based on a 6-h time integration of a column version of the GEOS moist physics with dynamical and other physical tendencies prescribed from a preliminary 3-h assimilation using the full GEOS DAS with conventional observations. The general procedure modifies vertical moisture and temperature profiles within observational and model uncertainties to minimize the least-square differences between the observed TPW and rainrates and those produced by the column model over the 6-h analysis window. The minimization yields constant moisture and temperature analysis tendencies, which are applied as additional forcing within the Incremental Analysis Update (IAU) framework of the GEOS DAS in the final 6-h assimilation cycle. Dynamic consistency is achieved through model integration during the assimilation cycle. Details of this "1+1" space-time dimension rainfall/TPW assimilation procedure and the basic features of the GEOS DAS are described in Hou et al. (2000a), with further improvements described in Hou et al. (2000b).

This 1+1D assimilation procedure, in its generalization to four dimensions, is related to the standard 4D variational assimilation but uses analysis increments instead of initial conditions as the control variable. In doing so, it effectively imposes the forecast model as a weak constraint in a manner similar to the variational continuous assimilation techniques (Derber 1989, Zupanski 1997). However, conceptually, the 1+1D scheme differs from most existing rainfall assimilation procedures in one important aspect - that it assimilates the time-averaged instead of instantaneous rainrates. The physical rationale is that the parameterized convection with implicit quasi-equilibrium assumptions is more consistent with a rainfall generation process that senses the atmospheric sounding over convective time scales of a few hours rather than instantaneous profiles. In practice, there is not sufficient rainfall observation to resolve the convective life cycles in the tropics, in the current implementation we use the 6-h analysis window for the averaging time as with all other data types used in the GEOS DAS.

An optimal use of TMI and SSMI rainfall and TPW observations in data assimilation requires detailed knowledge of observation and forecast model errors, which are both areas of active investigation. For a simple demonstration of the benefits of using these observations in assimilation, we will present results from a sub-optimal application of these data without using error specifications, as done in Hou et al. (2000b). The simplifying assumptions are: (i) the observed rainfall and TPW estimates are much more reliable than model-generated estimates, (ii) uncertainties in the moisture analysis are much larger than and uncorrelated with errors in the temperature field, and (iii) the moisture analysis increment has a prescribed vertically-decaying structure that mimics the Jacobian of the 6-h mean precipitation w.r.t. moisture perturbations and an amplitude constrained not to exceed the 6-h forecast error std dev against radiosonde data at any given level (see Hou, 2000b, for details). Under these conditions the general 1+1D scheme reduces to a two-parameter estimation problem to accommodate the 2 pieces of information provided by precipitation and TPW observations. This simplified 1+1D scheme shares a number of key assumptions with the physical initialization scheme (Krishnamurti et al. 1991, 1993) but differs in one important respect - it is implemented in the GEOS DAS to directly constrain the time-average rainrate and TPW over a 6-h analysis window, whereas physical initialization is typically used to improve the first guess by nudging the precipitation in the previous analysis cycle (Treadon 1996).

We performed a series of parallel assimilation experiments for two periods: one from 1 December 1997 to 31 January 1998, and the other from 1 June to 30 June 1998. The control is a standard GEOS assimilation with conventional observations that extends from 1 December 1997 through 30 June 1998. In four rainfall/TPW experiments we assimilated in each case, in addition to conventional observations, either the 6-h averaged TMI rainrates (TMI PCP assimilation), or TMI rainrates and TPW (TMI PCP+TPW assimilation), or TMI and SSM/I rainrates (TMI+SSMI PCP assimilation), or TMI and SSMI/I rainrates and TPW (TMI+SSMI PCP+TPW assimilation). Results from the TMI PCP and TMI PCP+TPW experiments have been reported separately in Hou et al. (2000b). The present article focuses on the two experiments using both TMI and SSM/I observations.

5. Impact on Time-Mean Fields

a. Surface precipitation

The impact of assimilating the 6-h averaged TMI and SSM/I rainrates on the GEOS precipitation field is illustrated in Fig. 1 for 0000 UTC on 23 January 1998. Figure 1a shows the combined 6-h, 2° x 2.5° gridded GPROF rainrates derived from the TMI and DMSP *F13* and *F14* SSM/I instruments. At this temporal and spatial resolution, there is some overlap between observations from the polar-orbiting DMSP satellites and the TRMM satellite at 35° orbit inclination. Errors in the assimilated tropical rainrates in the GEOS control, TMI+SSMI PCP assimilation, and TMI+SSMI PCP+TPW assimilation are shown in Figs. 1b, 1c, and 1d, respectively. Given at the top of each panel are the anomaly pattern correlation (AC), bias, and error std dev w.r.t. the combined TMI and SSM/I estimates, with the percentage changes relative to the GEOS control given in parentheses. (Note: the anomaly correlation refers to pattern correlation with the tropical mean removed.)

The statistics in Fig. 1 serve only as an illustration, as there is considerable variability in these 6-h error statsitcis. Typically, rainfall assimilation increases the pattern correlation from around 0.2 to 0.45-0.6 and reduces the error std dev by 15-20%. The addition of TPW data further increases the correlation to 0.6-0.7 and reduces std dev by 20-30% relative to the control.

The 1+1D assimilation algorithm is more effective in reducing the precipitation intensity than enhancing it in the GEOS DAS, leading to the negative tropical-mean biases in Figs. 1c and 1d, even though the errors are reduced locally. A plausible explanation for this asymmetry is that enhancing precipitation requires moistening of the lower troposphere, yet the high relative humidity in the tropical boundary layer limits, through saturation, the extent to which moisture analysis increments can moisten the low levels, while permitting a greater degree of drying to reduce precipitation.

The impact of rainfall and TPW assimilation on the monthly-mean tropical precipitation is summarized in Table 1 for January and June 1998, as verified against the gridded GPCP monthly-mean satellite-gauge estimate produced by Huffman et al. (1997). Results show that assimilating TMI and SSM/I rainrates increases the anomaly correlation from the 0.60-0.65 range

to 0.85-0.89, and reduces the error std dev by 41-48%. Figure 2 shows the improved precipitation fields for January 1998. Although rainrates derived from microwave channels tend to be less accurate over land than over oceans, Fig. 2c shows that assimilating the GPROF rainrates improves precipitation not only over oceans but over land as well. Figure 2d shows that using TPW data in conjunction with rainrate estimates yields further improvements. Similar results in terms of the overall impact of PCP+TPW assimilation for June 1998 is shown in the top right panel of Fig. 4.

b. Total precipitable water

The monthly-mean spatial statistics in Table 2 show that the 1+1D scheme is very effective in reducing errors in the assimilated TPW field. It virtually eliminates the monthly-mean spatial bias and reduces the error std dev by 75-80%. Assimilating TMI and SSM/I rainrates without TPW data also has a positive impact on TPW, mainly in reducing the tropical-mean bias. The improvements in the assimilated tropical TPW from PCP+TPW assimilation is shown in Fig. 4 (upper middle panels) for June 1998 using the combined gridded TMI+SSM/I Wentz retrievals as verification.

c. Verification against CERES/TRMM top-of-the-atmosphere radiation measurements

The TOA radiative flux measurements used in this study are the CERES/TRMM ERBE-like ES-4 2.5° x 2.5° gridded daily products interpolated onto the 2° x 2.5° GEOS model grids. For the tropics, the monthly-averaged bias is estimated to be ±1.5 Wm^{-2} for longwave (LW) fluxes and ±3 Wm^{-2} for shortwave (SW) fluxes, and the std dev is less than 3 Wm^{-2} for LW and 8.5 Wm^{-2} for SW (CERES/TRMM 1998). The GEOS DAS does not, at the present time, assimilate these observations, which may therefore be used as independent data to evaluate the impact of rainfall/TPW assimilation on the analysis. The bulk of the comparison of the analysis with CERES/TRMM observations will focus on January and June 1998.

Table 3 summarizes for January and June 1998 the spatial error statistics in OLR, OSR, and the total outgoing radiation (TOR = OLR+OSR) relative to CERES products *over all tropical*

locations where the month-mean rainfall has been modified by PCP+TPW assimilation by more than 1 mm d^{-1}. Results show that both OLR and OSR are significantly improved as a result of the improved precipitation: with tropical bias reductions in the range of 71-92%, and the std dev reductions between 42 and 48%. An example of these improvements is shown in Fig. 3 for the tropical OLR for January 1998. The error reductions in the TOR are somewhat less but still substantial. Table 3c shows bias reductions of 20-27% and std dev reductions of 17%, reflecting partial cancellations between OLR and OSR errors, which is not surprising as much of these errors are cloud-related, as we will show later in this section.

The benefits of rainfall/TPW assimilation is not limited to raining regions. Table 4 summarizes the improvements in OLR, OSR, and TOR averaged over the tropics for January and June 1998. The improved tropical OLR and OSR fields for June 1998 are shown in the two lower panels in Fig. 4. Assimilating TMI and SSM/I rainrates and TPW yields reductions in the error std dev of 41-44%, 30-39%, and 11-17% for OLR, OSR, and TOR, respectively. It also reduces the tropical-mean bias by 71-76% in OSR and 18-27% in TOR. The apparent increase in the tropical-mean bias in OLR is an artifact of the virtual elimination of the predominantly negative OLR bias over precipitating areas (see Table 3a and Fig. 3), leaving the tropical-mean bias being dominated by the positive biases in rain-free regions. The positive OLR bias in rain-free areas reflects a dry humidity bias in the lower troposphere, which is diminished by assimilating TPW observations, as evident in the comparison of the clear-sky OLR against CERES measurements in Table 5. About half of the 10 Wm^{-2} bias in the clear-sky OLR can be traced to the use of a high surface emissivity value in this version of the GEOS DAS, which has since been corrected in later versions. A smaller bias in the control would mean greater fractional improvements. The tropical bias in the clear-sky OSR is small in the GEOS control - about 1.0 Wm^{-2} for January and -0.7 Wm^{-2} for June (not shown) - well within observation uncertainty; rainfall/TPW assimilation has no significant impact on either its bias or error std dev.

Much of the errors in the GEOS OLR and OSR in the tropics are dominated by errors in clouds, the foregoing results suggest that assimilating precipitation and TPW data significantly improves the representation of clouds and cloud radiative effects in the analysis. This is confirmed by comparing the "cloud radiative forcing" (the difference between the clear-sky radiation and all-sky radiation) with CERES/TRMM estimates. The statistics in Table 6 show

large reductions in tropical-mean biases and std dev's in LW, SW, and net cloud forcing for January and June 1998. These improvements are dramatic, as illustrated in Fig. 5 for the tropical LW cloud radiative forcing. Clearly, improvements in precipitation has a direct impact on the distribution of clouds, which, in turn, improves the OLR and OSR. In fact, the spatial pattern correlations between the change in the January-mean tropical precipitation due to PCP+TPW assimilation and those in OLR and OSR (not shown) are -0.70 and 0.70, respectively. Note, however, that there is little correlation between the changes in precipitation and TOR due to large cancellations between the LW and SW effects of clouds.

One benefit of assimilating rainfall and TPW data is that they reduce state-dependent systematic errors in assimilation products. An example is given in Fig. 6, which compares the tropical OLR error std dev's in the GEOS control with those in the PCP+TPW assimilation for three averaging periods of 1, 5, and 30 days. The offsets between the control and PCP+TPW assimilation results are nearly constant in all three cases - ranging from 8.2 to 9.5 Wm^{-2}. Since the tropical mean is removed from the error std dev analysis, they likely represent reductions of spatially-varying, state-dependent systematic errors. Systematic error reduction is important in data assimilation since analysis algorithms typically assume unbiased observations and model forecasts, even though systematic errors in the forecasting model and analyses can be of the same order as the random components. Constraining the assimilation fields using precipitation and TPW data can compensate for systematic model errors (see Sec. 6c) and promote internal consistency of assimilation schemes.

The improvements in the outgoing radiation fluxes presented in this section derive mostly from the better spatial pattern information in the TMI and SSM/I precipitation data and are not sensitive to the intensity of the retrieved rainrates, as shown by the sensitivity experiments described in Hou et al. (2000a).

d. Impact on tropical latent heating, large-scale motions, and upper-tropospheric humidity

A primary goal of assimilating tropical precipitation data is to improve the 4D structure of latent heating and the associated large-scale circulation. A better latent heating distribution should improve not only the clouds and vertical velocities in raining areas but also the subsidence

in surrounding regions. Figure 7 shows that the time-mean changes in the divergent wind at 200 hPa, the omega vertical velocity at 500 hPa, and the upper tropospheric humidity (UTH) resulting from rainfall and TPW assimilation in January 1998 are tightly linked with the changes in precipitation. The spatial pattern correlation between the January-mean precipitation anomaly (Fig. 7a) and the vertical velocity anomaly at 500 hPa (Fig. 7b) is -0.89, and that between the specific humidity anomaly at 400 hPa (Fig. 7c) and the vertical velocity anomaly at 500 hPa is -0.62. However, the correlation between the *positive* (descending) omega velocity anomaly and the *negative* specific humidity anomaly is -0.78. The drying of the upper troposphere is thus directly linked to the enhanced subsidence resulting from rainfall/TPW assimilation. The changes in humidity at 400 hPa should represent an improvement in the UTH, which is not easy to confirm due to the lack of reliable observations. However, we can infer from the clear-sky OLR results in Table 5 that rainfall/TPW assimilation has a positive impact on the large-scale circulation and the UTH in clear-sky regions. In the next section, we further investigate the impact of rainfall/TPW assimilation on the UTH using radiance data from TOVS channels that are sensitive to the upper-level moisture.

e. Impact on upper-tropospheric moisture and temperature inferred from TOVS radiances

TOVS brightness temperature observations are used to assess the impact of rainfall/TPW assimilation on GEOS moisture and temperature analyses. Synthetic TOVS brightness temperatures were computed using GEOS temperature and humidity analyses and compared with brightness temperatures derived from the clear and cloud-cleared infrared radiances from the TOVS High-resolution Infrared Radiation Sounder 2 (HIRS2) and Microwave Sounding Unit (MSU). The HIRS cloud-cleared brightness temperatures were produced as a part of the Pathfinder Path A data set (Susskind et al. 1997). The procedure we used is described in Hou et al. (2000a). The absolute uncertainty of the synthetic minus observed brightness temperatures is estimated to be approximately 2 K, due to biases in observations and the radiative transfer model, which were not removed. Instead, we focus on the spatial structure of the brightness temperature residuals exceeding 2 K and the relative differences between the GEOS control and PCP+TPW assimilation.

In this section we examine results for 2 channels: The HIRS2 12 (6.7 μm), which is sensitive to the UTH and the MSU 2, which is sensitive to the mid-tropospheric temperature. HIRS2 12 has a peak sensitivity to UTH between about 300 and 500 hPa depending on local conditions. Figure 8 compares the synthetic HIRS2 12 and MSU 2 brightness temperatures with observations. The synthetic HIRS12 brightness temperature from the GEOS control shows a cold bias, reflecting a moist bias in UTH throughout the tropics. The difference in synthetic brightness temperature in the bottom left panel shows that rainfall/TPW assimilation leads to "warming" over much of the tropics and reductions of 6% in the bias and 11% in the error std dev w.r.t. observations. The spatial correlation between the *positive* synthetic brightness temperature anomaly and the *negative* specific humidity anomaly at 400 hPa (Fig. 7c) is -0.81. This is a result of an improved vertical motion field associated with improved precipitation in the assimilation, as shown earlier.

The MSU 2 has a relatively broad sensitivity to tropospheric temperature that peaks near 600 hPa and has a small sensitivity to surface emission. In Fig. 8 the top right panel shows that the synthetic MSU 2 brightness temperatures in the GEOS control are higher than the observed values, consistent with a warm bias in the temperature analysis. However, the differences may not be significant since they are less than the estimated uncertainty of 2 K. We can to some extent remove this ambiguity by examining the difference in synthetic brightness temperatures between two assimilation runs. The bottom right panel in Fig. 8 shows that the impact of rainfall/TPW assimilation is to reduce the warm biases by 0.05 to 0.2 K over large portions of the tropics, which is likely significant given the broad weighting function. Statistics show that rainfall/TPW assimilation reduces the tropical-mean bias by 4% and the error std dev by 7% w.r.t. the observed MSU 2 brightness temperatures.

6. Impact on Instantaneous Fields and Short-Range Forecasts

Forecast skills that result from an improved initial condition are used to assess the impact of rainfall and TPW assimilation on the instantaneous prognostic fields (i.e., temperature, winds, moisture, and surface pressure) in the GEOS analysis.

a. 5-day ensemble forecast

We performed parallel ensemble forecasts initialized with GEOS analyses with and without TMI and SSM/I data. Each ensemble consists of 12 independent samples of 5-day forecasts with initial conditions 5 days apart taken from two months of assimilation. For forecast verification, two analyses were used: (i) the operational analysis from the European Center for Medium-Range Weather Forecasts (ECMWF) and (ii) the average of the GEOS control and PCP+TPW analyses. Although the PCP+TPW analysis compares better with satellite observations than the control, as shown in Sec. 5, using the average of two analyses for verification removes biases associated with the initial conditions.

Figure 9a shows the rms error reductions in tropical 5-day forecasts of the 500 hPa geopotential height. Forecasts initialized with the PCP+TPW analysis yields smaller rms errors regardless which of the two verification analyses was used. Student's t test confirms that the forecast error reductions in the tropics are significant at the 99% level beyond 1 day in either case. In the extratropics, there was no statistically significant impact on the 5-day forecast.

Rainfall and TPW assimilation also reduces errors in the divergent component of horizontal winds in the tropics, as shown for the 200 hPa divergent meridional wind in Fig. 9b. The improvements are significant at the 99% level within the first 2 days, as verified against the ECMWF analysis. Figure 9c shows that rainfall/TPW assimilation also reduces the rms errors in the OLR in the first 2 days, as verified against the CERES/TRMM data, indicative of improved cloud fields, as discussed in Sec. 5.

b. Precipitation forecast

Figure 10 shows the impact of TMI and SSM/I rainfall/TPW assimilation on ensemble tropical precipitation forecast. The ensemble consisted of 20 cases of 3-day forecasts with initial conditions 3 days apart from the December 97 to January 98 period. Figure 10a shows that rainfall/TPW assimilation improves spatial correlation of the precipitation forecast with the GEOS PCP+TPW precipitation analysis. The greatest improvements occur within the first 24 hours, where the correlation coefficients are increased from 0.45 in the control to the 0.9-0.6 range. This

result is similar to what one obtains with physical initialization (Krisknamurti et al. 1994). The forecast improvement diminishes with the lead time presumably because the influence of a better initial condition is inherently limited by the growth of model errors. The improved spatial correlations shown in Fig. 10a are statistically significant at the 99% level for 66 forecast hours. By contrast, the reductions in the rms forecast errors shown in Fig. 10b are significant only within the first 24 hours. Rainfall/TPW assimilation thus appears to be more effective in improving the spatial patterns than the amplitudes of precipitation forecasts.

To investigate the local impact of rainfall/TPW assimilation, we examined the 6-hr average "observation minus forecast" (O-F) residuals at model gridboxes where TMI or SSM/I observations are available at both forecast verification times and the initial times from which forecasts were made with prognostic fields that had been modified by rainfall/TPW assimilation in the previous assimilation cycle. From the same 20 forecasts used for Fig. 10, we constructed 6-h O-F ensembles consisting of individual forecasts at those locations with improved initial conditions rather than averaged over all points in the tropics. In Table 7 the 6-h O-F precipitation forecast statistics for the first 45 hours show that forecasts from the PCP+TPW assimilation have much smaller biases for lead times longer 3 hours. (Results significant at the 99% level are italicized.) The lack of improvements in the first few hours is consistent with that rainfall/TPW assimilation is effective in reducing systematic errors, as discussed Sec. 5c, in which case there may be no detectable improvement in the initial period when the forecast errors are dominated by uncorrelated errors, which decay with time. By contrast, the fractional reductions in the error std dev, though significant, are marginally small. This is due in part to that the large std dev of the sub-sampled ensembles based on the spatially-limited, time-varying satellite observations available in a 6-h window. Nevertheless, it is significant that the forecasts are not degraded since internally consistent use of observations dictates that the improved analysis should improve, or at the very least, does not adversely affect forecast.

b. 6-hr observation minus forecast residuals

We computed the monthly-mean biases and error std dev's of the 6-hr O-F residuals for winds, geopotential height, and specific humidity averaged over tropical rawinsonde locations for

the GEOS control and PCP+TPW runs. Statistical tests show that rainfall and TPW assimilation affects mainly the O-F residuals for moisture but not the height or winds. Table 8 gives the moisture O-F biases and std dev's together with the "null hypothesis" probabilities that they are the same in the two cases. Results indicate that PCP+TPW assimilation decreases the std dev's of the moisture O-F residual between 300 and 500 hPa at the 1% probability level. The only significant change in bias occurs between 700 and 850 hPa, corresponding to a downward shift of the zero-bias level in the PCP+TPW case. Overall, these O-F's show that TMI+SSM/I rainfall/TPW assimilation reduces the moisture O-F residuals with no adverse impact on other fields, which is consistent with the TOVS brightness temperature results discussed in Sec. 5d.

7. Summary and discussion

This study shows that assimilating rainfall and TPW estimates derived from microwave instruments is very effective in improving the hydrological cycle and atmospheric energetics in the GEOS analysis - even with the limited observations available from a single TMI and 2 SSM/I instruments. It demonstrates that the microwave-based rainfall estimates, at their current levels of accuracy, are more reliable than model-based analyses, as substantiated using independent metrics based on the CERES/TRMM TOA radiation measurements. Results show that assimilating the 6-h averaged tropical TMI and SSM/I rainrates and TPW data reduces the state-dependent, systematic errors in assimilated data products. In particular, rainfall assimilation improves distributions of clouds and radiation in convective regions, as well as the latent heating and the associated large-scale circulation in the tropics, while TPW assimilation reduces moisture biases to improve the longwave radiation in clear-sky regions. An improved large-scale motion field also improves the upper tropospheric humidity, which is verified by comparing GEOS synthetic brightness temperatures for moisture-sensitive TOVS channels with observations.

Ensemble forecasts initialized with GEOS analyses with TMI and SSM/I rainfall and TPW data yield better 5-day forecasts of the 500 hPa geopotential height, and better 2-day forecasts of the 200 hPa divergent winds in the tropics. These forecast improvements indicate that rainfall/TPW assimilation improves not only the time-mean fields but also the instantaneous prognostic fields in the analysis. Rainfall/TPW assimilation also leads to improved 3-day

ensemble forecasts of precipitation, with the greatest improvements occurring in the first 24 hours, during which time the spatial correlations with observation-driven precipitation analyses increased from 0.45 in the control to the 0.9-0.6 range. This high correlation is not sustained beyond 1 day presumably because that improvements due to improved initial conditions are inherently limited by the growth of model errors. However, it is possible to achieve better results beyond 1 day using the multi-model super-ensemble approach used by Krishnamurti et al. (2000) to reduce the influence of systematic model errors. Examination of the 6-hr O-F statistics against TMI and SSM/I observations show that rainfall/TPW assimilation reduces spatial biases by roughly 50% in precipitation forecasts for lead times up to 3 days.

This work shows that assimilating TMI and SSM/I rainfall and TPW observations can substantially improve assimilated data even in a sub-optimal application without detailed error specifications. It may be possible to make even more effective use of these data through use of background and observation error covariance models. The results of this study provide a baseline for evaluating the performance of error covariance models. Rainfall/TPW assimilation experiments using the generalized 1+1D rainfall/TPW assimilation scheme will be reported in a subsequent paper.

While rainfall/TPW assimilation provides better initial conditions for short-range forecasts, it is worth noting that the improvements are even greater in the monthly-mean fields. In the presence of biases and other errors of the forecast model, forecast skills are not necessarily an accurate predictor of the improvements that can be achieved in time-averaged assimilation fields. These results suggest that assimilating rainfall and TPW data using the 1+1D scheme in the IAU framework can compensate for the systematic errors present in the forecast model. The analysis increments induced by rainfall and TPW data may be used to identify and correct the state-dependent errors in the forecast model using the empirical procedure described in DelSole and Hou (1999).

The present results are based on observations updated in 6-h assimilation cycles. The state-of-the-art assimilation systems, including the next-generation GEOS DAS, are evolving towards a time-continuous assimilation strategy to make better use of asynoptic observations from satellite platforms. Currently global analyses from different assimilation systems all suffer, to varying degrees, errors in clouds and precipitation in the tropics. This study suggests that

precipitation and TPW assimilation offers an effective means by which to improve the hydrological cycle and the related climate parameters in global analyses. Based on these results, we expect that the proposed Global Precipitation Mission to measure rainfall at high temporal and spatial resolution can provide a key observation type that will significantly improve the quality and utility of assimilated global datasets for climate analysis and weather forecasting applications.

Acknowledgments

It is a pleasure to acknowledge the support of this work by Dr. Ramesh Kakar, the TRMM Program Scientist, and Dr. Kenneth Bergman, Manager of Global Modeling and Analysis Program through NASA Grants 621-15-33-20, 622-24-27-20 and 291-04-15-20. We would like to thank Dr. Eric Nelkin for producing the gridded TMI and SSM/I GPROF rainrate estimates and performing the necessary quality control, and Dr. Joanna Joiner for making available the code for computing TOVS synthetic brightness temperatures.

REFERENCES

Adler, R., C. Kidd, M. Goodman, A. Ritchie,, R. Schudalla, G. Petty, M. Morrissey, and S. Greene, 1996: PIP-3 Intercomparison Results, Report of the PIP-3 Workshop, College Park, MD. [Available online from http://www.ghcc.msfc.nasa.gov/pip3].

Bell, T. L., A. Abdullah, R.L. Martin, and G.R. North, 1990: Sampling errors for satellite-derived tropical rainfall: Monte Carlo study using a space-time stochastic model. *J. Geophys. Res.*, 95, 2195-2205.

CERES/TRMM, 1998: CERES Data Products Catalog. Available online from http//:asd-www.larc.nasa.gov/ceres/trmm/ceres_trmm.html

Delsole, T., and A.Y. Hou, 1999: Empirical correction of a dynamic model: Part I. Fundamentals, *Mon. Wea. Rev.,* **127**, 2533-2545.

Derber, J.C., 1989: A variational continuous assimilation technique. *Mon. Wea. Rev.*, 117, 2437-2446.

Donner, L.J., 1988: An initialization for cumulus convection in numerical weather prediction models. *Mon. Wea. Rev.,* 116, 377-385.

Haddad, Z. S., E. A. Smith, C. D. Kummerow, T. Iguchi, M. R. Farrar, S. L. Durden, M. Alves, and W. S. Olson, 1997: The TRMM 'Day-1' Radar/Radiometer Combined Rain-Profiling Algorithm, *J. Meteor. Soc. Japan*, 75, 799-809.

Hou, A.Y., D. Ledvina, A. da Silva, S. Zhang, J. Joiner, R. Atlas, G. Huffman, and C. Kummerow, 2000a: Assimilation of SSM/I-derived surface rainfall and total precipitable water for improving the GEOS analysis for climate studies. *Mon Wea. Rev.*, **128**, 509-537.

-----, S. Zhang, A. da Silva, W. Olson, 2000b: Improving assimilated global data sets using TMI rainfall and columnar moisture observations. *J. Climate,* accepted.

Huffman, G.J., 1997: Estimates of root-mean-square random error contained in finite sets of estimated precipitation. *J. Appl. Meteor.*, 36, 1191-1201.

------, R. Adler, P. Arkin, A. Chang, R. Ferraro, A. Gruber, J. Janowiak, A. McNab, B. Rudolf, U. Schneider, 1997: The Global Precipitation Climatology Project (GPCP) Version 1 dataset. *Bull. Am. Meteorol. Soc.*, 78, 5-20.

Kasahara, A., A.P. Mizzi, and L.J. Donner, 1994: Diabatic initialization for improvement in the tropical analysis of divergence and moisture using satellite radiometric imagery data. *Mon. Wea. Rev.*, 120, 1360-1380.

Krishnamurti, T.N., K. Ingles, S. Cocke, R. Pasch, and T. Kitade, 1984: Details of low latitude medium range numerical weather prediction using a global spectral model II. Effect of orography and physical initialization. *J. Meteor. Soc. Japan*, 62, 613-649.

------, J. Xue, H.S. Bedi, K. Ingles, and O. Oosterhof, 1991: Physical initialization for numerical weather prediction over the tropics. *Tellus*, 43AB, 53-81.

------, H.S. Bedi, and K. Ingles, 1993: Physical initialization using SSM/I rain rates. *Tellus*, 45A, 247-269.

------, C.M. Kishtawal, D.R. Bachiochi, Z. Zhang, T.E. Larow, C.E. Williford, S. Gadgil, and S. Surendran, 2000: Multi-model superensemble forecasts for weather and seasonal climate. *Meteoro. and Atmos. Phyiscs*, submitted.

Kummerow, C., W. Olson, and L. Giglio, 1996: A simplified scheme for obtaining precipitation and vertical hydrometeor profiles from passive microwave sensors. *IEEE Trans. Geosci Remote Sensing*, 34, 1213-1232.

------, et al. (27 authors), 2000: The Status of Tropical Rainfall Measuring Mission (TRMM) after 2 years in orbit. J. Appl. Meteoro., submitted.

Newman, M., P.D. Sardeshmukh, and J.W. Bergman, 2000: An assessment of the NCEP, NASA, and ECMWF reanalyses over the tropical west Pacific warm pool. *Bull. Am. Meteorol. Soc.*, 81, 41-48.

Olson, W.S., C.D. Kummerow, G.M. Heymsfield, and L. Giglio, 1996: A method for combined passive-active microwave retrievals of cloud and precipitation profiles. *J. Appl. Meteor.*, 35, 1763-1789.

Pierdicca, N., F. S. Marzano, P. Basili, P. Ciotti, G. d'Auria, and A. Mugnai, 1996: Precipitation retrieval from spaceborne microwave radiometers based upon multivariate analysis of simulated cloud-radiation datasets. *IEEE Trans. Geosci. Remote Sens.*, 34, 1-16.

Puri, K., and M. J. Miller, 1990: The use of satellite data in the specification of convective heating for diabatic initialization and moisture adjustment in numerical weather prediction

models. *Mon. Wea. Rev.*, 118, 67-93.

Remote Sensing Systems (RSS), 2000: Description of TMI and SSM/I data products. Available online from http://www.ssmi.com, Remote Sensing Systems, Santa Rosa, Calif.

Sorooshian, S., K. Hsu, and X. Gao, 1999: Tropical rain estimation over the Pacific region using geostationary imagery combined with the TRMM rain data. Preprints of the 3rd International Scientific Conference on the Global Energy and Water Cycle, 16-19 June, Beijing, China.

Susskind, J., P. Piraino, L. Rokke, L. Iredell, and A. Mehta, 1997: Characteristics of the TOVS pathfinder path A data set, *Bull. Am. Meteorol. Soc.*, 78, 1449-1472.

Treadon, R.E., 1996: Physical initialization in the NMC global data assimilation system. Meteor. Atmos. Phys., 60, 57-86.

TRMM, 1996: Scientific Operations Plan, NASA Goddard Space Flight Center, Greenbelt, MD, 122 pp. [Available online from http://trmm.gsfc.nasa.gov].

TRMM Data Assimilation at NASA Goddard, 2000: http://dao.gsfc.nasa.gov/ScienceEfforts/Highlights/TRMM.

Tsuyuki, T., 1996a: Variational data assimilation in the tropics using precipitation data. Part I: Column model. *Meteor. Atmos. Phys.*, 60, 87-104.

-----, 1996b: Variational data assimilation in the tropics using precipitation data. Part II: 3D model. *Mon. Wea. Rev.*, 124, 2545-2561.

-----, 1997: Variational data assimilation in the tropics using precipitation data. Part III: Assimilation of SSM/I precipitation rates. *Mon. Wea. Rev.*, 125, 1447-1464.

Turpeinen, O.M., L. Garand, R. Benoit, and M. Roch, 1990: Diabatic initialization of the Canadian regional finite-element (RFE) model using satellite data. Part I: methodology and application to a winter storm. *Mon. Wea. Rev.*, 118, 1381-1395.

World Climate Research Program (WCRP), 1998: Proceedings of the First WCRP International Conference on Reanalyses. October 27-31, Silver Spring, MD, 461 pp.

Wentz F. J., 1997: A well-calibrated ocean algorithm for SSM/I, *J. Geophys. Res.*, Vol. 102, No. C4, 8703-8718.

Zupanski, D., 1997: A general weak constraint applicable to operational 4DVAR data assimilation systems. *Mon. Wea. Rev.*, 125, 2274-2292.

-----, and F. Mesinger, 1995: Four-dimensional variational assimilation of precipitation data. *Mon. Wea. Rev.*, 123, 1112-1127.

Table 1

Monthly-mean spatial statistics of GEOS tropical precipitation against GPCP satellite-gauge estimate

	January 1998					June 1998				
	AC	bias (mm d^{-1})		std dev (mm d^{-1})		AC	bias (mm d^{-1})		std dev (mm d^{-1})	
GEOS Control	0.7	-0.1	-	3.24	-	0.6	0.75	-	3.67	-
PCP Assimilation	0.8	-0.47	*	2.24	-31%	0.8	0	*	2.28	-38%
PCP+TPW Assim.	0.9	-0.51	*	1.92	-41%	0.9	-0.4	*	1.92	-48%

*See text for the apparent increase in bias.

Table 2

Monthly-mean spatial statistics of GEOS TPW over tropical oceans against Wentz estimate

	January 1998					June 1998				
	AC	bias (g cm^{-2})		std dev (g cm^{-2})		AC	bias (g cm^{-2})		std dev (g cm^{-2})	
GEOS Control	0.9	-0.3	-	0.45	-	1	-0.3	-	0.36	-
PCP Assimilation	1	-0.2	-36%	0.43	-4%	1	-0.2	-44%	0.43	-20%
PCP+TPW Assim.	1	0	-97%	0.09	-80%	1	0	-99%	0.091	-75%

Table 3a

Monthly-mean spatial statistics of GEOS OLR against CERES/TRMM ERBE-like ES-4 estimate over tropical locations where the monthly-mean rainfall has been modified by more than 1 mm d^{-1}

	January 1998					June 1998				
	AC	bias (Wm^{-2})		std dev (Wm^{-2})		AC	bias (Wm^{-2})		std dev (Wm^{-2})	
GEOS Control	0.5	-18	-	28.2	-	0.5	-24	-	30.4	-
PCP Assimilation	0.8	-5.6	-70%	16.3	-42%	0.8	-5.5	-78%	17.9	-41%
PCP+TPW Assim.	0.9	2	-83%	14.7	-48%	0.8	1.82	-92%	17.3	-43%

Table 3b

Monthly-mean spatial statistics of GEOS OSR against CERES/TRMM ERBE-like ES-4 estimate over tropical locations where the monthly-mean rainfall has been modified by more than 1 mm d^{-1}

	January 1998					June 1998				
	AC	bias (Wm^{-2})		std dev (Wm^{-2})		AC	bias (Wm^{-2})		std dev (Wm^{-2})	
GEOS Control	0.5	32	-	33.6	-	0.5	39.3	-	39.4	-
PCP Assimilation	0.8	18.9	-41%	20.2	-40%	0.8	18.8	-52%	22.7	-43%
PCP+TPW Assim.	0.9	9.39	-71%	19.5	-42%	0.8	9.19	-77%	20.7	-48%

Table 3c

Monthly-mean spatial statistics of GEOS total outgoing radiation against CERES/TRMM ERBE-like ES-4 estimate over tropical locations where the monthly-mean rainfall has been modified by more than 1 mm d^{-1}

	January 1998					June 1998				
	AC	bias (Wm^{-2})		std dev (Wm^{-2})		AC	bias (Wm^{-2})		std dev (Wm^{-2})	
GEOS Control	0.5	15.2	-	18.5	-	0.5	15.1	-	20.9	-
PCP Assimilation	0.6	13.7	-10%	16.3	-12%	0.7	3.73	-75%	18.3	-12%
PCP+TPW Assim.	0.7	12.2	-20%	15.3	-17%	0.6	11	-27%	17.3	-17%

Table 4a

Monthly-mean spatial statistics of GEOS tropical OLR against CERES/TRMM ERBE-like ES-4 estimate

	January 1998					June 1998				
	AC	bias (Wm^{-2})		std dev (Wm^{-2})		AC	bias (Wm^{-2})		std dev (Wm^{-2})	
GEOS Control	0.7	2.75	-	26.1	-	0.6	-2.72	-	28.7	-
PCP Assimilation	0.9	7.21	*	17.9	-31%	0.9	4.53	*	17.5	-39%
PCP+TPW Assim.	0.9	10.8	*	14.5	-44%	0.9	7.84	*	15.1	-41%

*See text for the apparent increase in bias.

Table 4b

Monthly-mean spatial statistics of GEOS tropical OSR against CERES/TRMM ERBE-like ES-4 estimate

	January 1998					June 1998				
	AC	bias (Wm^{-2})		std dev (Wm^{-2})		AC	bias (Wm^{-2})		std dev (Wm^{-2})	
GEOS Control	0.7	16.1	-	32	-	0.6	19.9	-	36.6	-
PCP Assimilation	0.8	10.8	-33%	23.9	-25%	0.7	11.7	-41%	25.4	-30%
PCP+TPW Assim.	0.8	4.67	-71%	22.5	-30%	0.8	4.69	-76%	22.3	-39%

Table 4c

Monthly-mean spatial statistics of GEOS tropical total outgoing radiation against CERES/TRMM ERBE-like ES-4 estimate

	January 1998					June 1998				
	AC	bias (Wm^{-2})		std dev (Wm^{-2})		AC	bias (Wm^{-2})		std dev (Wm^{-2})	
GEOS Control	0.6	18.9	-	21.7	-	0.7	17.2	-	23.4	-
PCP Assimilation	0.7	18	-4%	20.3	-7%	0.8	9.22	-46%	21.2	-10%
PCP+TPW Assim.	0.7	15.5	-18%	19.3	-11%	0.8	12.5	-27%	19.4	-17%

Table 5
Monthly-mean spatial statistics of GEOS clear-sky OLR over tropical oceans
against CERES/TRMM ERBE-like ES-4 estimate

	January 1998					June 1998				
	AC	bias (Wm^{-2})		std dev (Wm^{-2})		AC	bias (Wm^{-2})		std dev (Wm^{-2})	
GEOS Control	0.8	10.3	-	5.58	-	0.8	11.4	-	4.1	-
PCP Assimilation	0.8	9.56	-7%	5.45	-2%	0.8	9.78	-14%	4.22	+3%
PCP+TPW Assim.	0.9	8.56	-17%	4.66	-17%	0.9	8.55	-25%	3.06	-25%

Table 6a
Monthly-mean spatial statistics of GEOS LW cloud forcing over tropical oceans
against CERES/TRMM ERBE-like ES-4 estimate

	January 1998					June 1998				
	AC	bias (Wm^{-2})		std dev (Wm^{-2})		AC	bias (Wm^{-2})		std dev (Wm^{-2})	
GEOS Control	0.7	985	-	22.6	-	0.7	14.3	-	27.8	-
PCP Assimilation	0.9	5.4	-37%	14.3	-37%	0.8	6.54	-54%	15.3	-45%
PCP+TPW Assim.	0.9	-0.6	-51%	11.1	-51%	0.8	0.77	-95%	12.8	-54%

Table 6b
Monthly-mean spatial statistics of GEOS SW cloud forcing over tropical oceans
against CERES/TRMM ERBE-like ES-4 estimate

	January 1998					June 1998				
	AC	bias (Wm^{-2})		std dev (Wm^{-2})		AC	bias (Wm^{-2})		std dev (Wm^{-2})	
GEOS Control	0.4	-28	-	38.2	-	0.3	-32.2	-	42.6	-
PCP Assimilation	0.5	-18	-36%	28.3	-26%	0.5	-19.6	-39%	28.6	-33%
PCP+TPW Assim.	0.6	-11	-62%	25.8	-32%	0.5	-11.8	-63%	24.6	-42%

Table 6c
Monthly-mean spatial statistics of GEOS net cloud forcing over tropical oceans
against CERES/TRMM ERBE-like ES-4 estimate

	January 1998					June 1998				
	AC	bias (Wm^{-2})		std dev (Wm^{-2})		AC	bias (Wm^{-2})		std dev (Wm^{-2})	
GEOS Control	0.4	-16	-	24.5	-	0.4	-13.6	-	24.8	-
PCP Assimilation	0.5	-13	-19%	22.9	-6%	0.4	-11.7	-14%	23.9	-4%
PCP+TPW Assim.	0.5	-9.2	-41%	21.9	-11%	0.5	-7.12	-48%	20.5	-17%

Table 7
Local impact of rainfall and TPW assimilation on 6-h O-F statistics
for tropical precipitation forecasts verified against TMI+SSM/I observations

Forecast Time	3 h	9 h	15 h	21 h	27 h	33 h	39 h	45 h
Sample Size	42160	44762	42541	52870	42272	45266	42387	49920
	bias							
Control PCP+TPW Assim.	0.535 0.708	*0.882* *0.485*	*0.758* *0.014*	*1.304* *0.477*	*1.210* *0.480*	*1.450* *0.814*	*1.184* *0.588*	*1.356* *0.950*
% change t prob	+32% 0.07	***-45%*** ***$1e^{-4}$***	***-98%*** ***$4e^{-13}$***	***-63%*** ***$1e^{-16}$***	***-60%*** ***$5e^{-15}$***	***-44%*** ***$1e^{-10}$***	***-50%*** ***$4e^{-9}$***	***-30%*** ***$1e^{-5}$***
	error std dev							
Control PCP+TPW Assim.	*14.45* *13.35*	15.34 15.16	15.02 14.90	*16.32* *16.13*	*13.69* *13.39*	*15.02* *14.76*	*14.87* *14.63*	14.85 14.76
% change F prob	***-7.6%*** ***$1e^{-16}$***	-1.2% 0.012	-0.8% 0.078	***-1.2%*** ***0.009***	***-2.2%*** ***$3e^{-6}$***	***-1.7%*** ***$2e^{-4}$***	***-1.6%*** ***0.001***	-0.6% 0.180

Table 8
Specific humidity O-F residuals against rawinsonde data (30°S to 30°N, January 1998)

Pressure (hPa)	bias			error std dev		
	Control	PCP+TPW	t-test prob	Control	PCP+TPW	F-test prob
300	-0.0840	-0.0771	0.2601	***0.0817***	***0.0380***	***9.811×10^{-5}***
400	-0.1566	-0.1196	0.0363	***0.2243***	***0.1670***	***1.571×10^{-6}***
500	-0.1470	-0.1295	0.5081	***0.3464***	***0.2795***	***3.342×10^{-4}***
700	***0.0332***	***-0.1905***	***7.462×10^{-5}***	0.6870	0.6400	0.2368
850	***0.5591***	***0.2568***	***4.492×10^{-3}***	1.2777	1.1523	0.0945
1000	-0.9933	-0.8497	0.4078	1.3697	1.3949	0.8385

Figure captions

Figure 1. (a) Six-hour averaged GPROF rainrates based on observations from the TMI and *F13* and *F14* SSM/I instruments at 0000 UTC on 23 January 1998. The satellite observation tracks are shaded. The light shading denotes either no precipitation or rainrates less than 2 mm day^{-1}. (b) Difference between GPROF rainrates and precipitation from the GEOS control sampled at TMI and SSM/I observation locations. Shown at the top of the panel are tropical-mean spatial statistics of the GEOS precipitation w.r.t. the TMI and SSM/I observations. (c) Same as (b) but for the assimilation using TMI and SSM/I rainrates without TPW retrievals. The percentage error reduction relative to the control is given in parentheses. (d) Same as (c) but for the assimilation using TMI and SSM/I rainrates in conjunction with TPW data.

Figure 2. (a) Monthly-mean combined satellite-gauge GPCP precipitation estimate for January 1998. (b) Difference between the GPCP estimate and precipitation from the GEOS control, with tropically-averaged spatial correlations and error statistics. (c) Same as (b) but for the TMI+SSMI PCP assimilation. The percentage change in error std dev relative to the control is given in parentheses. (d) Same as (c) but for the TMI+SSMI PCP+TPW assimilation.

Figure 3. OLR comparison against CERES/TRMM measurements at locations where precipitation has been modified by more than 1 mm d^{-1} for January 1998. (a) Difference between the GEOS control and CERES/TRMM, with tropical-mean spatial correlations and error statistics. (b) Same as (a) but for TMI PCP assimilation. The percentage changes in bias and error std dev relative to the control are given in parentheses. (c) Same as (b) but for the TMI+SSMI PCP assimilation. (d) Same as (c) but for the TMI+SSMI PCP+TPW assimilation.

Figure 4. Impact of rainfall/TPW assimilation on the monthly-mean tropical precipitation, TPW, OLR, and OSR as verified against observations. for June 1998. Left panels show errors in the GEOS control assimilation. Right panels show the corresponding errors in the TMI+SSM/I rainfall and TPW assimilation. Percentage changes relative to errors in the control are given in parentheses. See text for discussion of bias values accompanied by an asterisk.

Figure 5. Improvements in the longwave "cloud radiative forcing" as verified against CERES/TRMM observations for January and June 1998. Percentage reductions in the spatial bias and error std dev relative to the control are given in parentheses.

Figure 6. Tropically-averaged error std dev in OLR as a function of averaging periods of 1, 5, and 30 days for the first 30 days in January 1998.

Figure 7. (a) Change in precipitation between PCP+TPW assimilation and the control for January, 1998. Superimposed are the changes in the horizontal divergent wind vector at 200 hPa. (b) Change in the omega velocity at 500 hPa. The anomaly correlation between this and changes in precipitation shown in (a) is -0.89. (c) Changes specific humidity at 400 hPa. The anomaly correlation between this and changes in 500 hPa omega velocity is -0.62.

Figure 8. Comparison of GEOS synthetic HIRS2 channel 12 and MSU channel 2 brightness temperatures with observations for January, 1998. Percentage reductions in the spatial bias and error std dev relative to the control are given in parentheses.

Figure 9. Impact of TMI+SSM/I rainfall and TPW assimilation on 5-day ensemble forecasts. (a) Forecast rms error in tropical geopotential height at 500 hPa, as verified against the ECMWF analysis and the GEOS TMI+SSMI PCP+TPW analysis. (b) Same as (a) except for the 200 hPa divergent meridional wind verified against the ECMWF analysis. (c) Same as (b) except for the OLR verified against the CERES/TRMM observations.

Figure 10. Impact of TMI+SSM/I rainfall and TPW assimilation on 3-day ensemble precipitation forecasts. (a) Spatial correlation with tropical precipitation from the GEOS TMI+SSMI PCP+TPW assimilation. (b) The corresponding rms error.

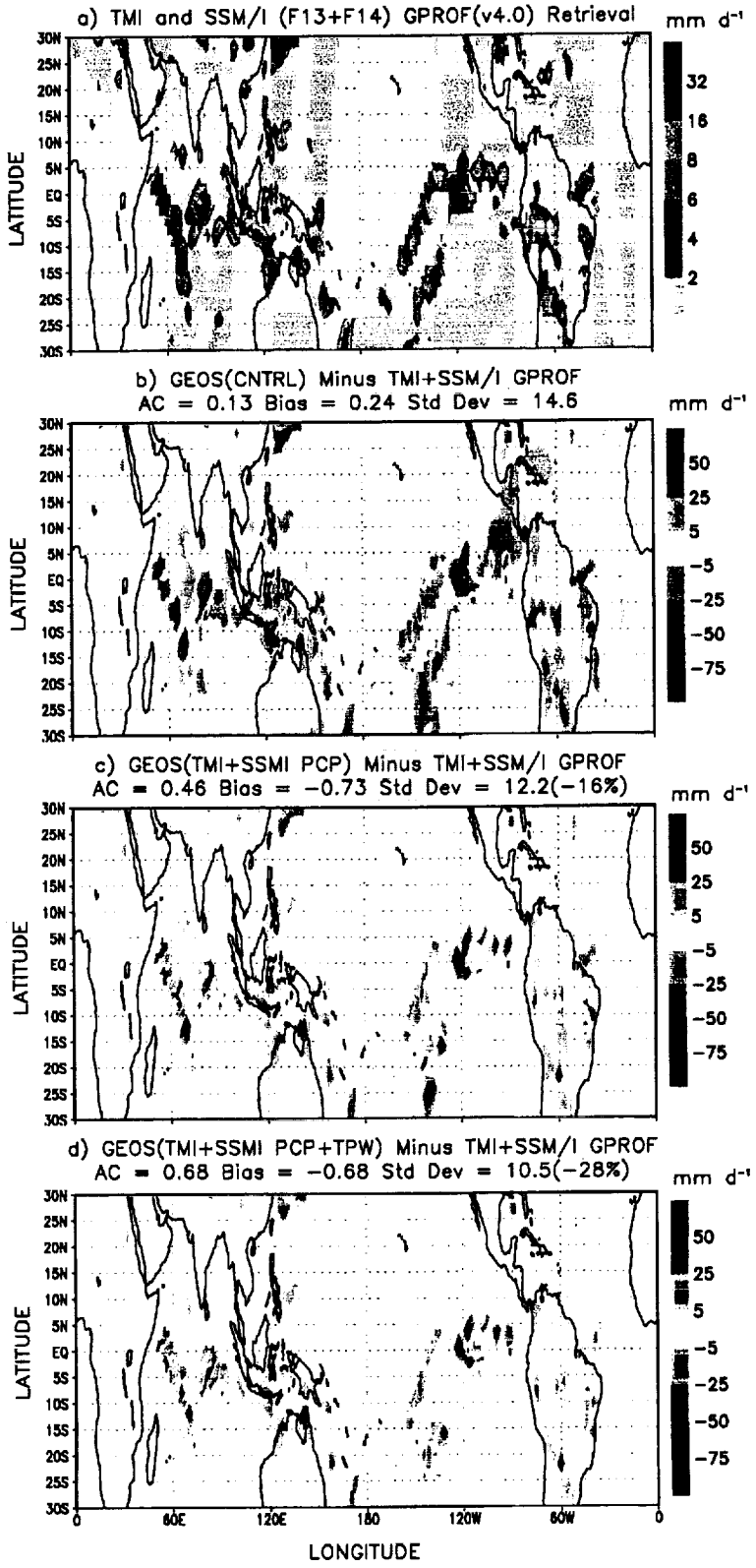
Impact of Rainfall and TPW Assimilation on Precipitation at
TMI+SSM/I Observation Locations: 0000 UTC 23 January 1998
a) TMI and SSM/I (F13+F14) GPROF(v4.0) Retrieval
mm d⁻¹
32
16
8
6
4
2
b) GEOS(CNTRL) Minus TMI+SSM/I GPROF
AC = 0.13 Bias = 0.24 Std Dev = 14.6
mm d⁻¹
50
25
5
-5
-25
-50
-75
c) GEOS(TMI+SSMI PCP) Minus TMI+SSM/I GPROF
AC = 0.46 Bias = -0.73 Std Dev = 12.2(-16%)
mm d⁻¹
50
25
5
-5
-25
-50
-75
d) GEOS(TMI+SSMI PCP+TPW) Minus TMI+SSM/I GPROF
AC = 0.68 Bias = -0.68 Std Dev = 10.5(-28%)
mm d⁻¹
50
25
5
-5
-25
-50
-75
LATITUDE
30N
25N
20N
15N
10N
5N
EQ
5S
10S
15S
20S
25S
30S
0
60E
120E
180
120W
60W
0
LONGITUDE

Fig. 1

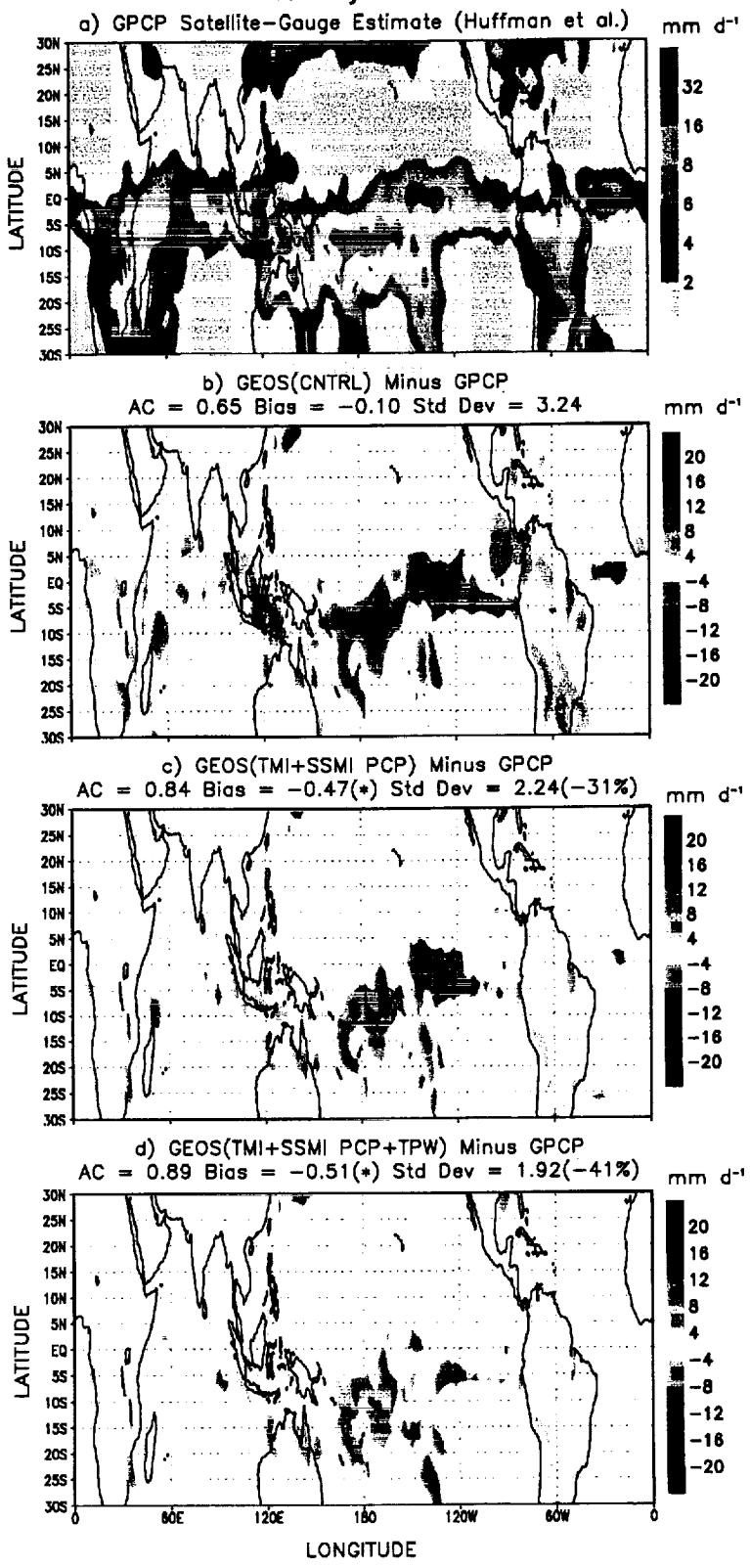
Impact of Rainfall and TPW Assimilation on Precipitation
January 1998
a) GPCP Satellite-Gauge Estimate (Huffman et al.)
mm d⁻¹
32
16
8
6
4
2
b) GEOS(CNTRL) Minus GPCP
AC = 0.65 Bias = −0.10 Std Dev = 3.24
mm d⁻¹
20
16
12
8
4
−4
−8
−12
−16
−20
c) GEOS(TMI+SSMI PCP) Minus GPCP
AC = 0.84 Bias = −0.47(*) Std Dev = 2.24(−31%)
mm d⁻¹
20
16
12
8
4
−4
−8
−12
−16
−20
d) GEOS(TMI+SSMI PCP+TPW) Minus GPCP
AC = 0.89 Bias = −0.51(*) Std Dev = 1.92(−41%)
mm d⁻¹
20
16
12
8
4
−4
−8
−12
−16
−20
LATITUDE
30N
25N
20N
15N
10N
5N
EQ
5S
10S
15S
20S
25S
30S
0
60E
120E
180
120W
60W
0
LONGITUDE

Fig. 2

OLR Improvements Associated with Rainfall Changes > 1 mm d^{-1}
at TMI+SSM/I Observation Locations: January 1998

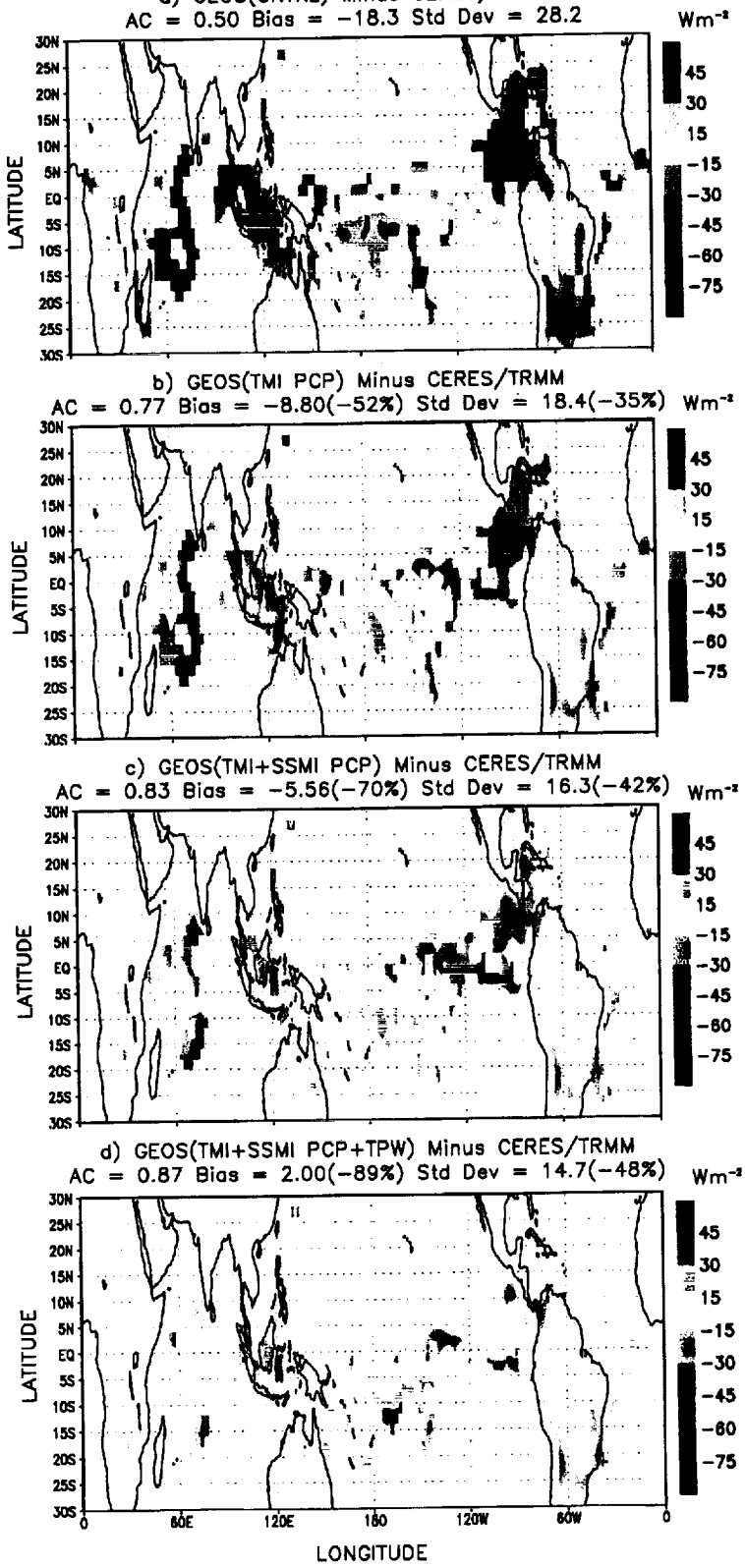

Fig. 3

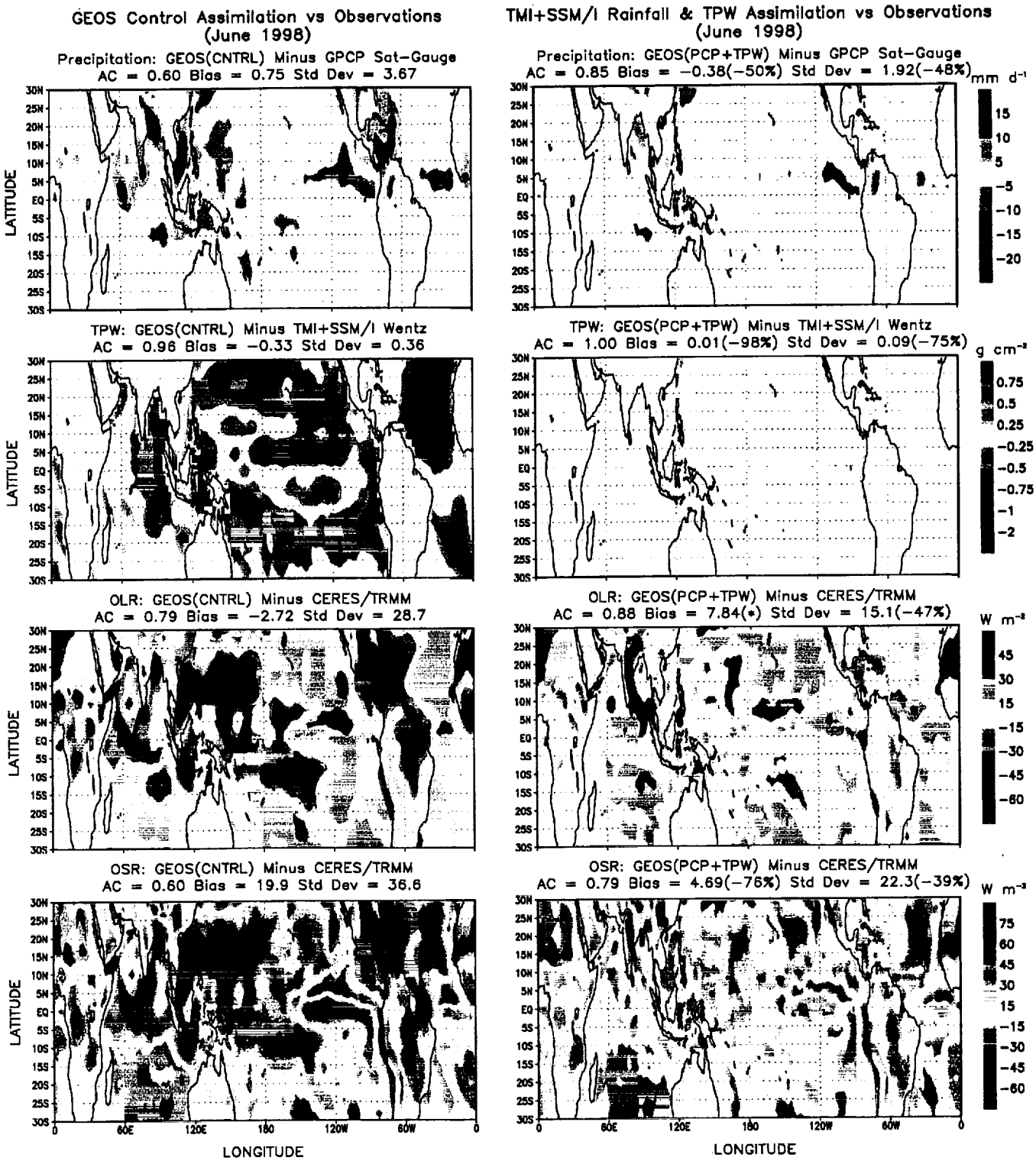
GEOS Control Assimilation vs Observations
(June 1998)
Precipitation: GEOS(CNTRL) Minus GPCP Sat-Gauge
AC = 0.60 Bias = 0.75 Std Dev = 3.67
TPW: GEOS(CNTRL) Minus TMI+SSM/I Wentz
AC = 0.96 Bias = −0.33 Std Dev = 0.36
OLR: GEOS(CNTRL) Minus CERES/TRMM
AC = 0.79 Bias = −2.72 Std Dev = 28.7
OSR: GEOS(CNTRL) Minus CERES/TRMM
AC = 0.60 Bias = 19.9 Std Dev = 36.6
TMI+SSM/I Rainfall & TPW Assimilation vs Observations
(June 1998)
Precipitation: GEOS(PCP+TPW) Minus GPCP Sat-Gauge
AC = 0.85 Bias = −0.38(−50%) Std Dev = 1.92(−48%)
mm d⁻¹
15
10
5
−5
−10
−15
−20
TPW: GEOS(PCP+TPW) Minus TMI+SSM/I Wentz
AC = 1.00 Bias = 0.01(−98%) Std Dev = 0.09(−75%)
g cm⁻²
0.75
0.5
0.25
−0.25
−0.5
−0.75
−1
−2
OLR: GEOS(PCP+TPW) Minus CERES/TRMM
AC = 0.88 Bias = 7.84(*) Std Dev = 15.1(−47%)
W m⁻²
45
30
15
−15
−30
−45
−60
OSR: GEOS(PCP+TPW) Minus CERES/TRMM
AC = 0.79 Bias = 4.69(−76%) Std Dev = 22.3(−39%)
W m⁻²
75
60
45
30
15
−15
−30
−45
−60
LATITUDE
30N
25N
20N
15N
10N
5N
EQ
5S
10S
15S
20S
25S
30S
0
60E
120E
180
120W
60W
LONGITUDE

Fig. 4

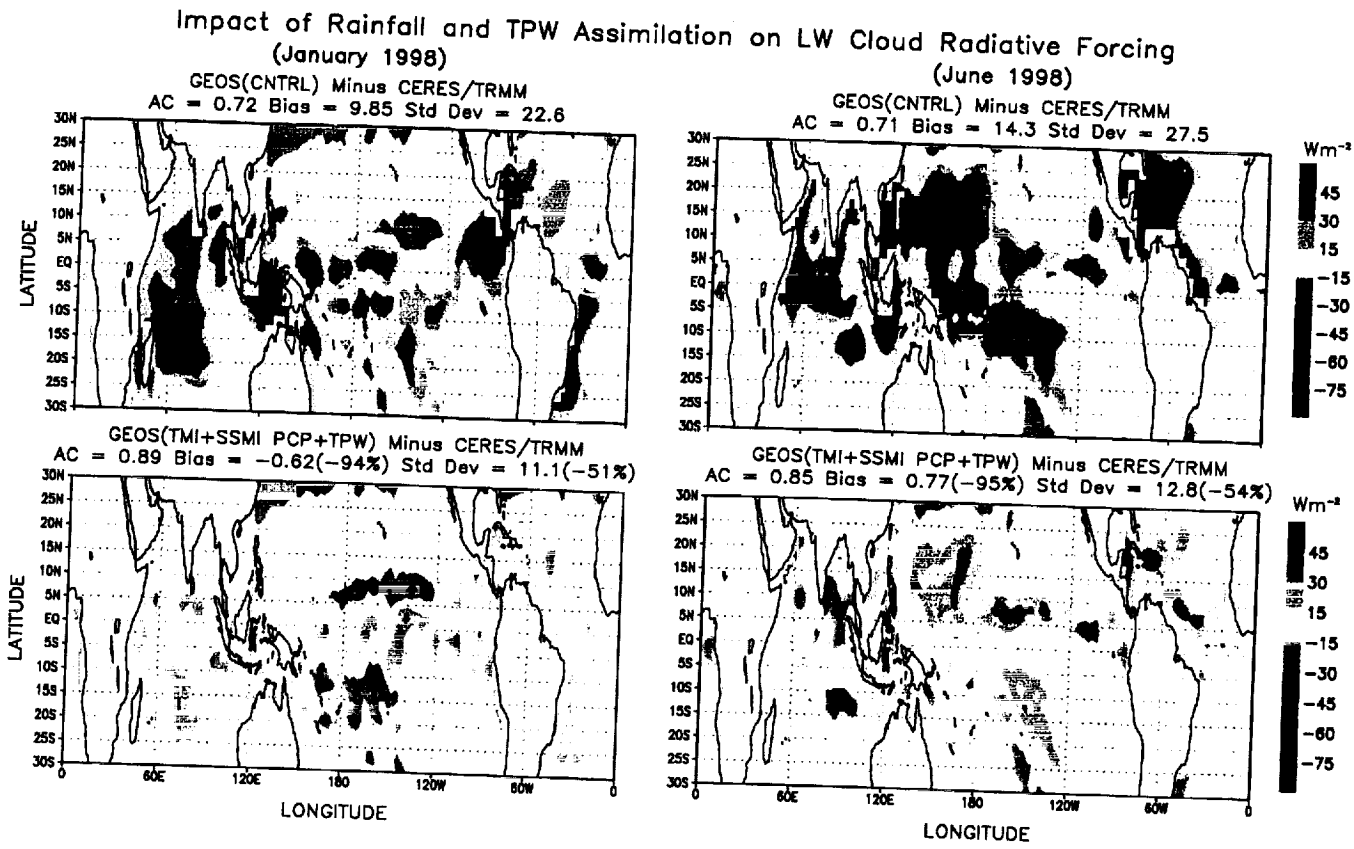
Impact of Rainfall and TPW Assimilation on LW Cloud Radiative Forcing
(January 1998)
GEOS(CNTRL) Minus CERES/TRMM
AC = 0.72 Bias = 9.85 Std Dev = 22.6
GEOS(TMI+SSMI PCP+TPW) Minus CERES/TRMM
AC = 0.89 Bias = −0.62(−94%) Std Dev = 11.1(−51%)
LATITUDE
LONGITUDE
(June 1998)
GEOS(CNTRL) Minus CERES/TRMM
AC = 0.71 Bias = 14.3 Std Dev = 27.5
GEOS(TMI+SSMI PCP+TPW) Minus CERES/TRMM
AC = 0.85 Bias = 0.77(−95%) Std Dev = 12.8(−54%)
Wm⁻²
45
30
15
−15
−30
−45
−60
−75

Fig. 5

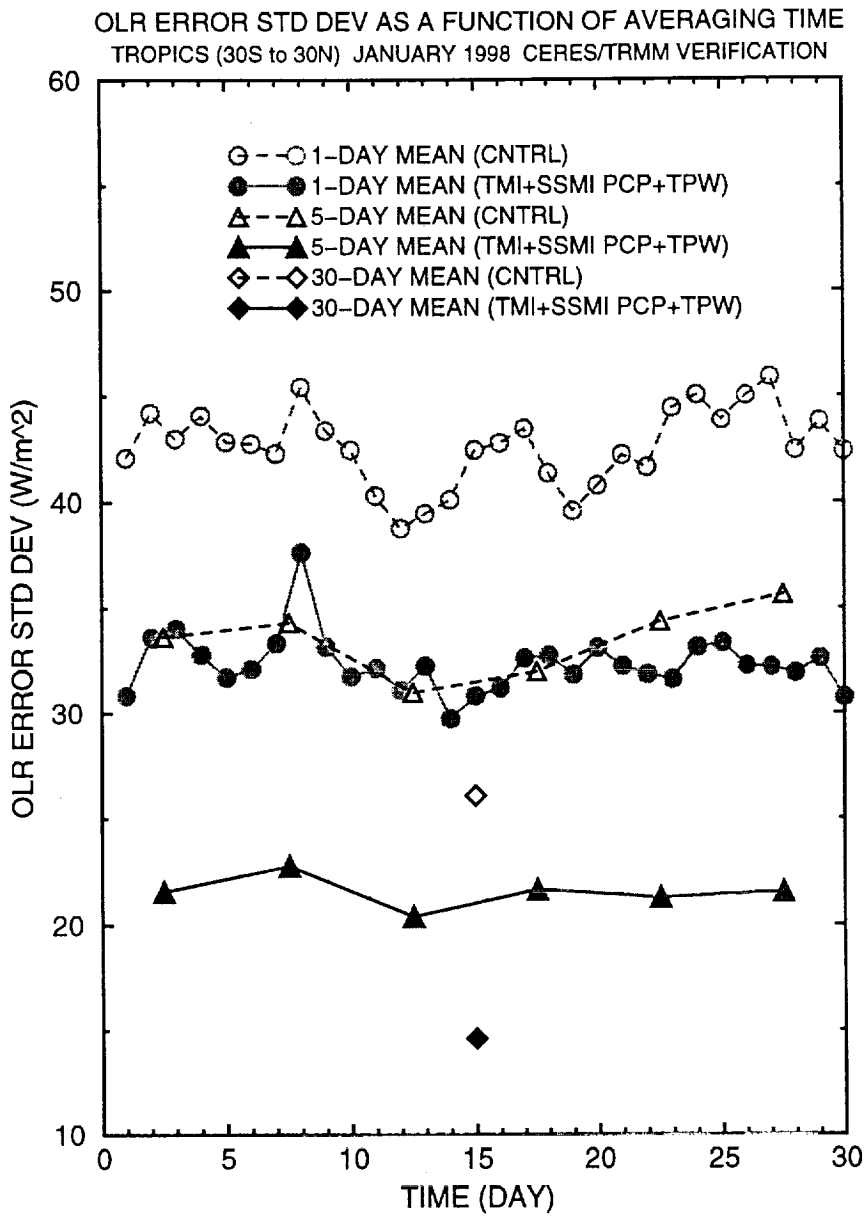
OLR ERROR STD DEV AS A FUNCTION OF AVERAGING TIME
TROPICS (30S to 30N) JANUARY 1998 CERES/TRMM VERIFICATION
1-DAY MEAN (CNTRL)
1-DAY MEAN (TMI+SSMI PCP+TPW)
5-DAY MEAN (CNTRL)
5-DAY MEAN (TMI+SSMI PCP+TPW)
30-DAY MEAN (CNTRL)
30-DAY MEAN (TMI+SSMI PCP+TPW)
OLR ERROR STD DEV (W/m^2)
TIME (DAY)
60
50
40
30
20
10
0
5
10
15
20
25
30

Fig. 6

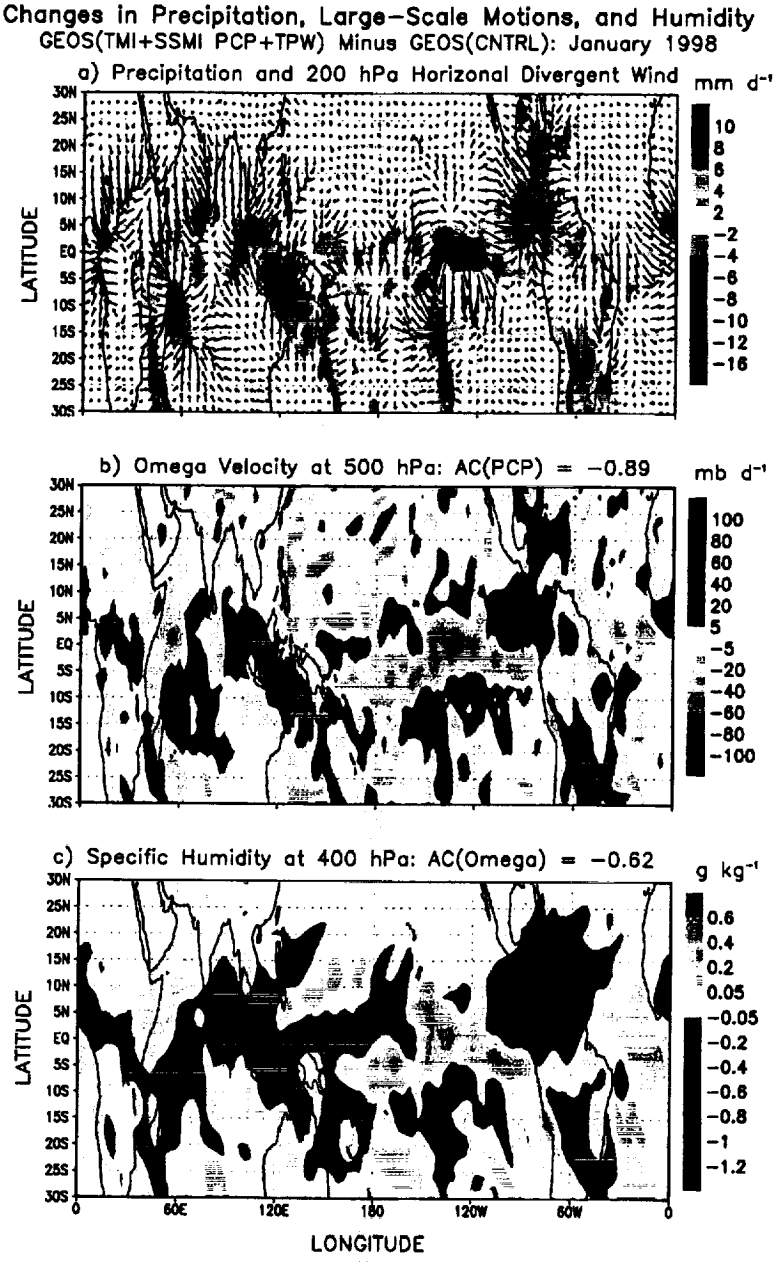
Changes in Precipitation, Large-Scale Motions, and Humidity
GEOS(TMI+SSMI PCP+TPW) Minus GEOS(CNTRL): January 1998
a) Precipitation and 200 hPa Horizonal Divergent Wind
mm d⁻¹
10
8
6
4
2
-2
-4
-6
-8
-10
-12
-16
b) Omega Velocity at 500 hPa: AC(PCP) = -0.89
mb d⁻¹
100
80
60
40
20
5
-5
-20
-40
-60
-80
-100
c) Specific Humidity at 400 hPa: AC(Omega) = -0.62
g kg⁻¹
0.6
0.4
0.2
0.05
-0.05
-0.2
-0.4
-0.6
-0.8
-1
-1.2
LATITUDE
30N
25N
20N
15N
10N
5N
EQ
5S
10S
15S
20S
25S
30S
0
60E
120E
180
120W
60W
0
LONGITUDE

Fig. 7

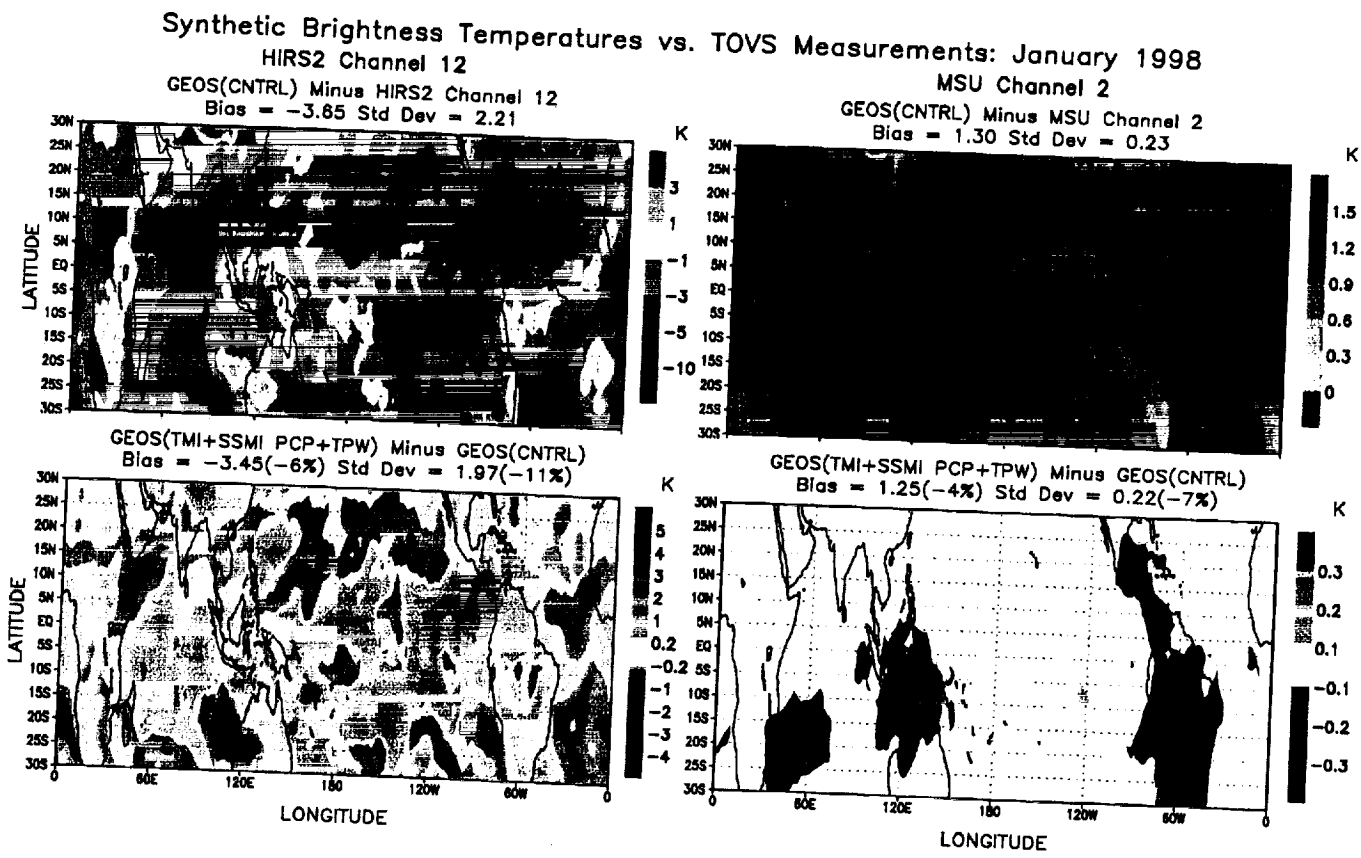
Synthetic Brightness Temperatures vs. TOVS Measurements: January 1998
HIRS2 Channel 12
GEOS(CNTRL) Minus HIRS2 Channel 12
Bias = −3.65 Std Dev = 2.21
MSU Channel 2
GEOS(CNTRL) Minus MSU Channel 2
Bias = 1.30 Std Dev = 0.23
GEOS(TMI+SSMI PCP+TPW) Minus GEOS(CNTRL)
Bias = −3.45(−6%) Std Dev = 1.97(−11%)
GEOS(TMI+SSMI PCP+TPW) Minus GEOS(CNTRL)
Bias = 1.25(−4%) Std Dev = 0.22(−7%)
LATITUDE
LONGITUDE
K

Fig. 8

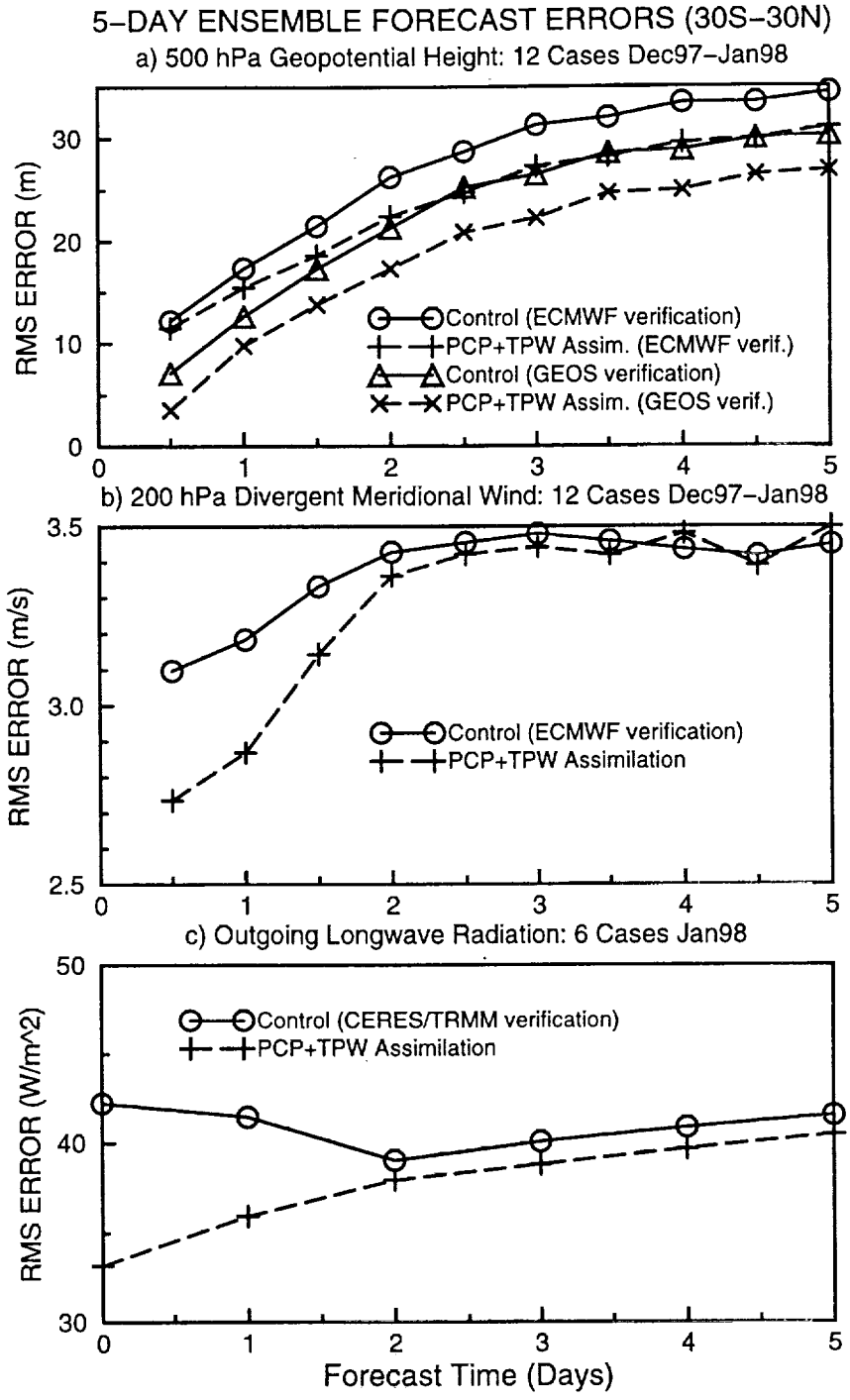
5-DAY ENSEMBLE FORECAST ERRORS (30S-30N)
a) 500 hPa Geopotential Height: 12 Cases Dec97-Jan98
RMS ERROR (m)
0
10
20
30
0
1
2
3
4
5
Control (ECMWF verification)
PCP+TPW Assim. (ECMWF verif.)
Control (GEOS verification)
PCP+TPW Assim. (GEOS verif.)
b) 200 hPa Divergent Meridional Wind: 12 Cases Dec97-Jan98
RMS ERROR (m/s)
2.5
3.0
3.5
Control (ECMWF verification)
PCP+TPW Assimilation
c) Outgoing Longwave Radiation: 6 Cases Jan98
RMS ERROR (W/m^2)
30
40
50
Control (CERES/TRMM verification)
PCP+TPW Assimilation
Forecast Time (Days)

Fig. 9

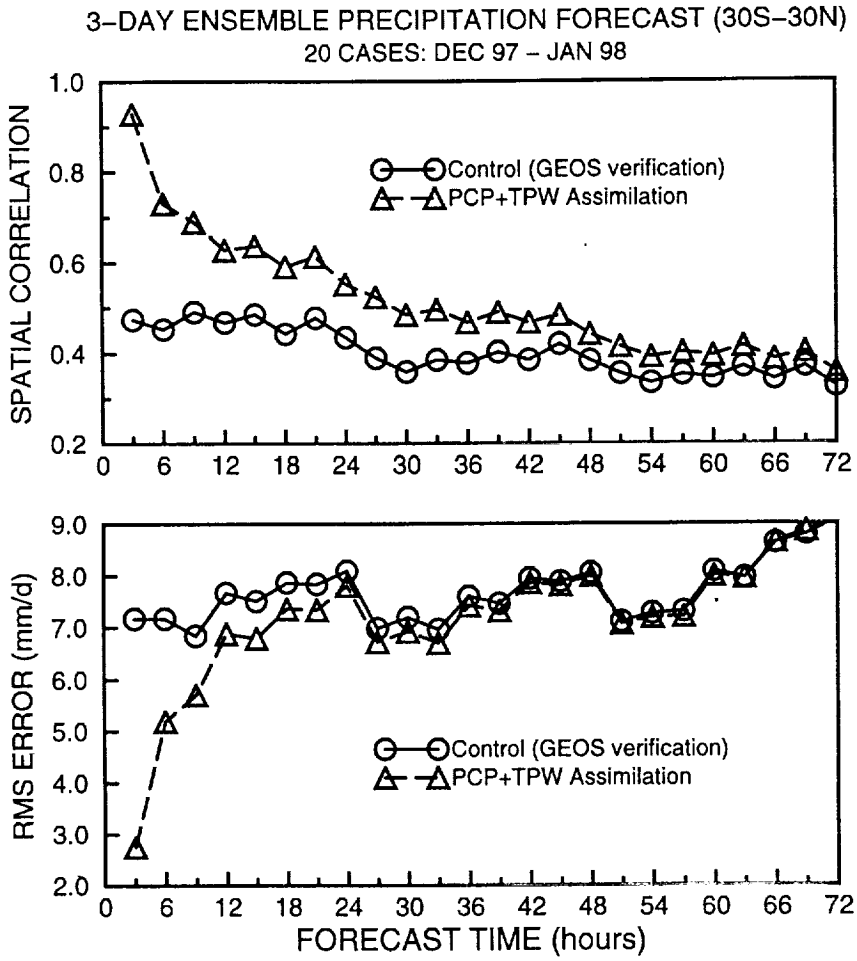
3–DAY ENSEMBLE PRECIPITATION FORECAST (30S–30N)
20 CASES: DEC 97 – JAN 98
SPATIAL CORRELATION
1.0
0.8
0.6
0.4
0.2
Control (GEOS verification)
PCP+TPW Assimilation
0 6 12 18 24 30 36 42 48 54 60 66 72
RMS ERROR (mm/d)
9.0
8.0
7.0
6.0
5.0
4.0
3.0
2.0
Control (GEOS verification)
PCP+TPW Assimilation
0 6 12 18 24 30 36 42 48 54 60 66 72
FORECAST TIME (hours)

Fig. 10